Gasification of woody biomass

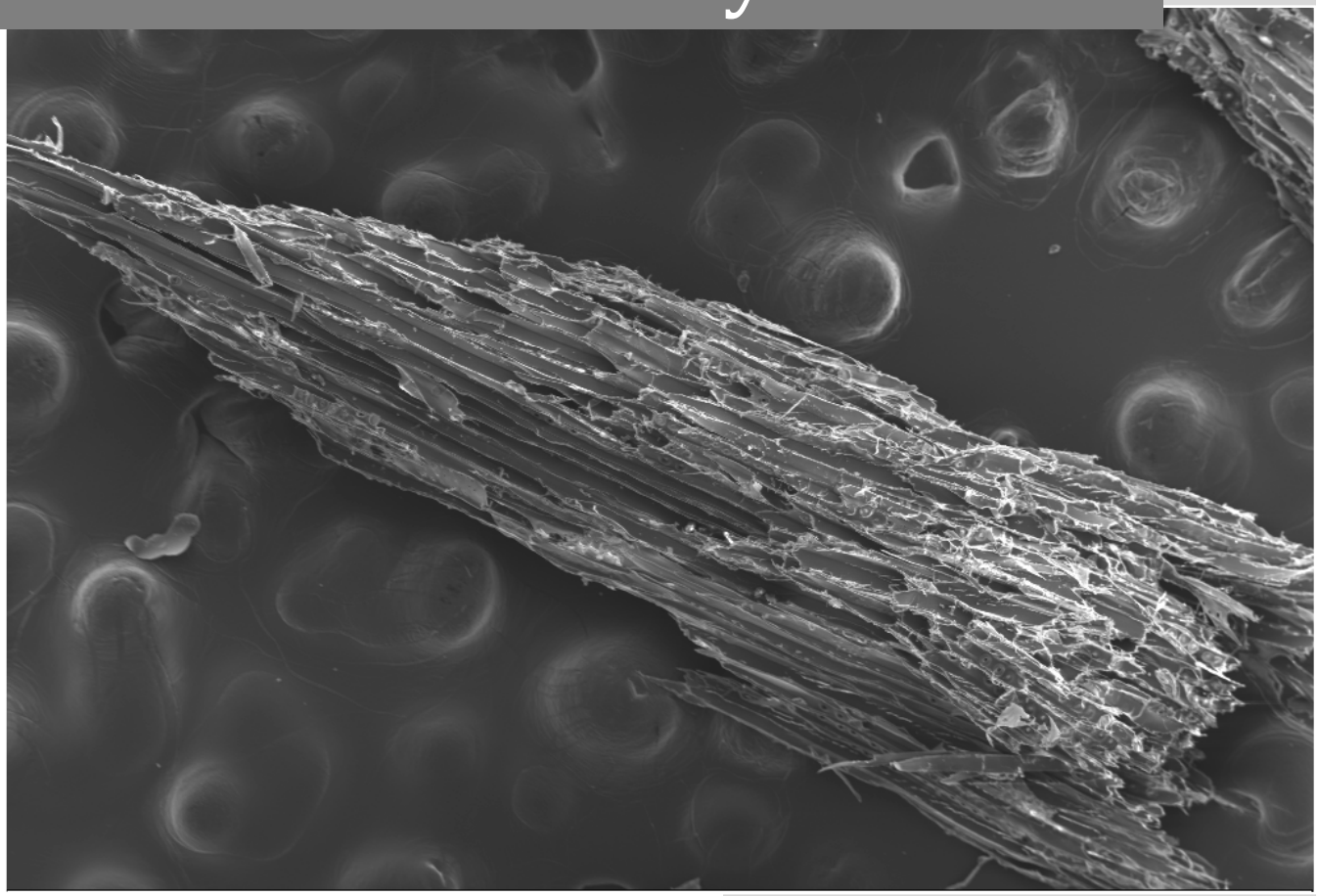

Tessa Jansen (s0140600)

University of Twente

Internship at SINTEF Energi AS

January 2011 - April 2011

Supervisor SINTEF Energi AS:

Judit Sandquist

Supervisor University of Twente:

Stefan Luding

Preface

This report is the result of the internship I conducted early 2011 at SINTEF Energi AS.

After applying, e-mailing and some waiting it became clear that Judit Sandquist and Berta Matas Guell (both part of the bio energy group within SINTEF Energi AS) were inviting me to work together with them, for which I am grateful. So on Wednesday 19th of January 2011 I got into the plane towards Trondheim, Norway and after some housing struggles, I could start with the internship.

The project which I was a (small) part of is GasBio (gasification for biofuels). The main objectives of this project are to develop Norwegian competence in the biofuels area and to contribute to the reduction of biofuel production costs. So I would be working on biomass gasification and perform thermo gravimetric analysis (TGA) experiments to examine the influence of gasification parameters on the gasification process. Therefore, I have carried out micro-scale (TGA) experiments to assist in the efforts to find the best gasification technology and conditions for project activities later on.

Furthermore, this internship has helped me to achieve some personal goals and gain experience. For example, I worked on a totally new topic in a working environment, did experiments and lived abroad for slightly over three months. Even including some experimental struggles, this internship was a really valuable experience to me, from which I have learned a lot. Judit and Berta, thank you for your scientific, experimental and social support during my internship. And Stefan, thank you for your 'digital' support.

Abstract

Influence of heating rate on the gasification process and char reactivity has been investigated by performing multiple gasification, pyrolysis and combustion experiments, using a thermogravimetric analyzer, Fourier transform infrared radiation analyzer and a mass spectrometer.

When applying a higher heating rate, delays in weight loss were noted both in combustion, pyrolysis and gasification. Cause of this delay is expected to be heat and mass transfer limitations, but other causes cannot be eliminated.

The char gasification process contained two weight loss stages not belonging to the gasification process. The first is expected to be caused by influence of desorption phenomena, for the second stage no convincing explanation was found, but it is sure this stage is not a part of the gasification reactions. The main gasification stage, both in char and direct gasification, was characterized by a weight loss that got smaller when there was less weight left (reduced reaction speed with increasing conversion). When lowering the gasification temperature, the gasification reaction decreased much in speed. By comparing gasification in one or two steps, it showed that the gasification stage in the two steps process took a little longer, indicating further structural development of the char during cooling down after char production.

Char reactivity has been examined by scanning electron microscope (SEM) pictures, char combustion experiments and gasification experiments. Char gasification clearly showed higher heating rate char to be more reactive. After some irreproducible experiments, also char combustion resulted in the same conclusion. From the SEM pictures it was suggested that the high heating rate char was likely to be more reactive. It can be concluded that in all examined situations char produced at a higher heating rate is more reactive than lower heating rate char.

Introduction

Producing fuels from biomass has become more important in recent years. Climate changes and the influence of carbon dioxide emission, as an important greenhouse gas, have been recognized by large parts of the world. The security of supply of fossil fuels becomes more difficult, since they are mainly mined in unstable regions worldwide, moreover they are depleting. This supports the need for research in the use of renewable energy sources like biomass.

Via gasification of biomass, a hydrogen and carbon monoxide rich gas, called syngas (synthesis gas), can be produced. This syngas can be used for various applications like the production of biofuels via Fischer-Tropsch synthesis, electricity production via turbines and the production of various chemicals. This report focuses on the influence of various parameters in the gasification process for the purpose of producing biofuels from woody biomass.

For this purpose, first the characteristics of biomass feedstock are discussed. The main components, structure and the standard characterization of biomass samples are addressed (section 1). In section 2, three thermal conversion processes, pyrolysis, combustion and gasification are discussed, including the products created during these processes. Furthermore, the process of producing biofuels from syngas, Fischer-Tropsch synthesis, is addressed briefly and the influence of various parameters on the gasification process is covered.

In the experimental part, section 3, three devices have been used, a thermo gravimetric analyzer (TGA), a Fourier transform infrared radiation (FTIR) analyzer and a mass spectrometer (MS). The operation, possible results and connection of the three devices are covered. Moreover, the experiments conducted are addressed in section 4 and their results and the most interesting comparisons are discussed (section 5).

Finally, a conclusion will be drawn and some recommendations will be given in section 6.

Table of Contents

1 Woody biomass

The feedstock used in this study is woody biomass. In this section structure, main components and characterization of woody biomass samples is discussed.

1.1 Structure

Wood is composed of elongated cells, tracheids, most of which are oriented in the longitudinal direction of the stem. Their functions are liquid transportation, storage and transportation of food supply and providing mechanical strength to the wood. Separate tracheids are connected by pits, openings that function as valves to be able to control the water flow and prevent air and vapour bubbles to get into the liquid flow. Also horizontal orientated cells, perpendicular to the main direction of the stem, are present in the wood structure, like for example perpendicular rays. Softwoods (like spruce) and hardwoods (like birch or beech) are two classes of wood, both contain these structures. (Figure 1.1, Figure 1.2) [1]

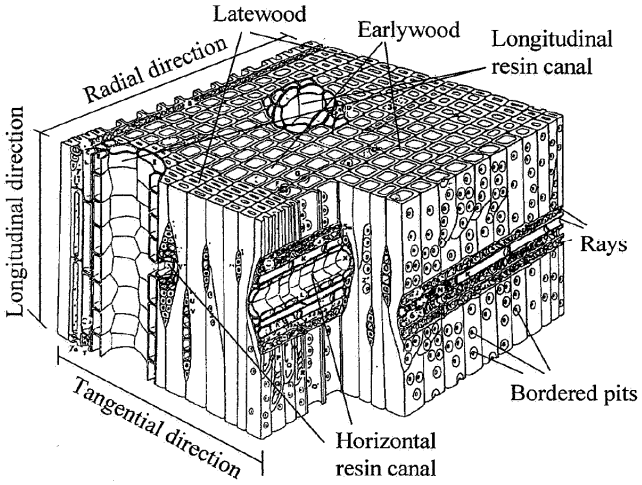

FIGURE 1.1 GROSS STRUCTURE OF SOFTWOOD [1]

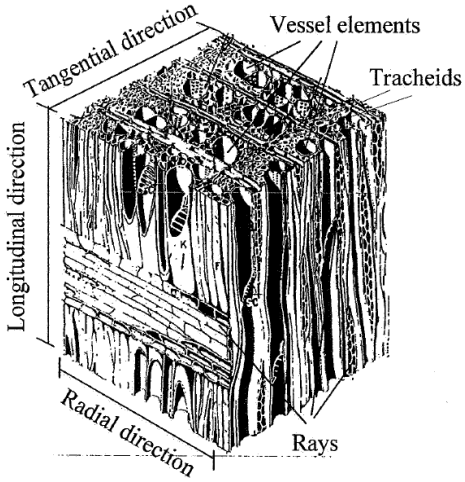

FIGURE 1.2 GROSS STRUCTURE OF HARDWOOD [1]

1.2 Components

Woody biomass has three main components: cellulose, hemicellulose and lignin. Cellulose is the component of woody biomass which gives structure to the wood and is the main component of cell walls, Figure 1.3. Hemicellulose, Figure 1.4, is also present in cell walls and lignin, Figure 1.5, with an aromatic structure (rings of carbon with alternating double and single bonds), acts as a binding agent. [2]

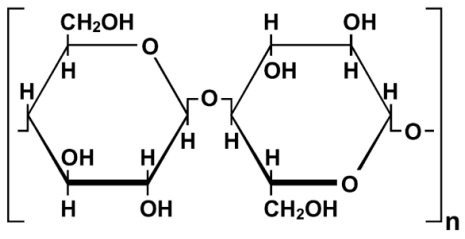

FIGURE 1.3 CELLULOSE [3]

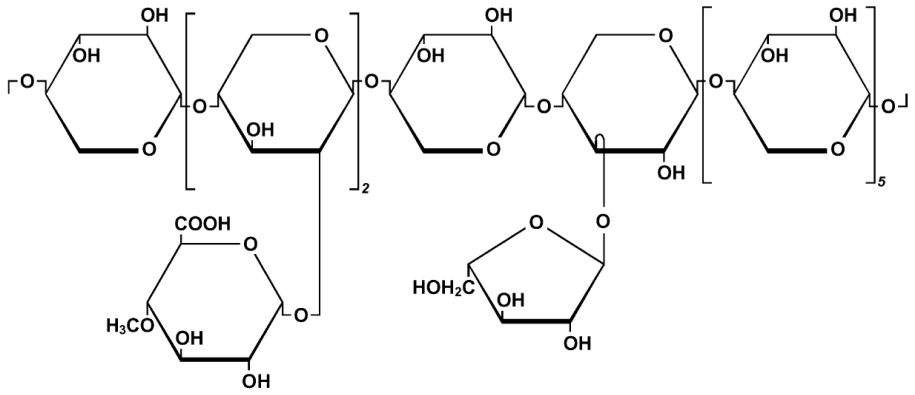

FIGURE 1.4 HEMICELLULOSE [3]

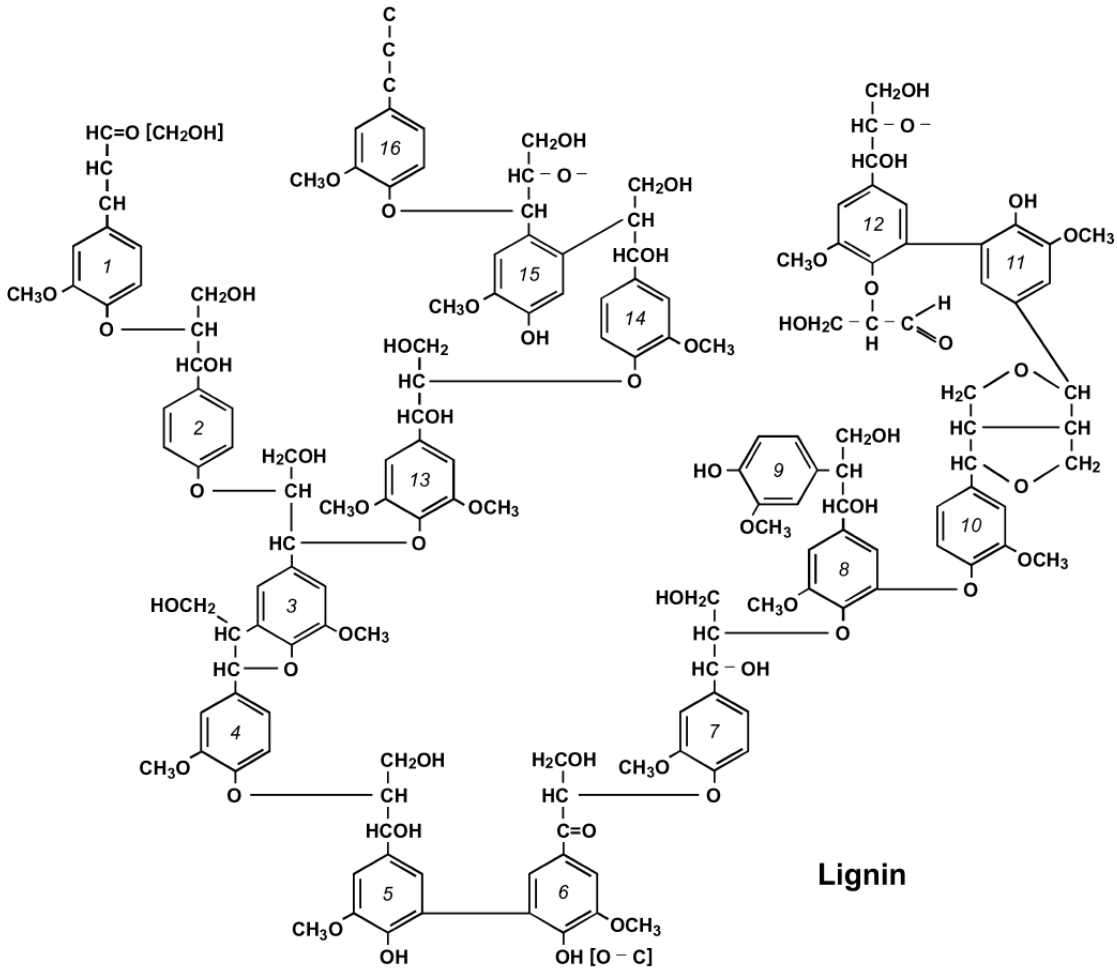

FIGURE 1.5 MODEL OF SPRUCE LIGNIN [3]

Various types of wood contain different amounts of these three basic components, hardwood types contain more hemicelluloses than softwood types, for some examples of compositions are presented in Table 1.1. A difference in composition results in another behaviour during thermal conversion processes, because the different components have a different reactivity (section 3.1).

TABLE 1.1 COMPOSITION OF WOODY BIOMASS IN WEIGHT PERCENTAGE [2]

Tree species	*Cellulose*	*Hemicellulose*	*Lignin*
Beech	45.2	32.7	22.1
White birch	44.5	36.6	18.9
Red maple	44.8	31.2	24.0
Eastern white cedar	48.9	20.4	30.7
Eastern hemlock	45.2	22.3	32.5
Jack pine	45.0	26.4	28.6
White spruce	48.5	21.4	27.1

Generally the composition of biomass feedstock can be expressed as [4]:

$$C_x H_y O_z$$

For a wide range of biomass feedstock, the molar ratios of carbon, hydrogen and oxygen do not vary much. Therefore this composition of biomass is often used: [2]

$$CH_{1.4}O_{0.6}$$

A wood sample used during experiments is usually characterized by proximate and ultimate analysis. Unfortunately, no characterization of the spruce sample used in this study is available; therefore both will be briefly discussed below.

1.2.1 Proximate analyses

A proximate analysis determines the moisture content, volatile matter content, ash content and fixed carbon content of a sample.

Every sample contains some moisture; especially biomass (compared to fossil fuels) can have a large and varying moisture content. By heating the sample to relatively low temperatures (~110 °C) the moisture content evaporates. When moisture evaporation is completed, all water has been removed from the sample and the sample is called dry. Moisture content (moist) is usually reported on a wet basis (wb) in weight percentage: [2]

$$Y_{moist}^{wb} = (wet\ weight - dry\ weight)/wet\ weight$$

The volatile matter (VM) content consists of components which are released from the sample at temperatures until ~900°C in the absence of air and is usually reported on a dry base (db): [2]

$$Y_{VM}^{db} = weight\ loss/dry\ weight$$

Ash content is determined by the weight of the sample after complete combustion: [2]

$$Y_{ash}^{db} = weight\ ash/dry\ weight$$

Finally, fixed carbon (FC) is determined by: [2]

$$Y_{FC}^{db} = 1 - Y_{VM}^{db} - Y_{ash}^{db}$$

1.2.2 Ultimate analysis

During ultimate analysis the chemical composition and the heating value of a sample are determined. In the chemical composition usually the weight percentages of carbon, hydrogen, oxygen, nitrogen,

sulphur and ash are given. From this composition the heating value, a measure for the amount of energy that can be obtained from a sample, can be determined experimentally or calculated via an empirical relation. [2]

Ultimate analysis is not used in this study and will therefore not be discussed further. More information about ultimate analysis can be found in “Energy from biomass” by Bastiaans, Oijen, Prins [2].

2 Thermal conversion processes

Gasification is one of the four thermo-chemical biomass conversion processes for energy purposes, together with pyrolysis, combustion and liquefaction. [2] All conversion processes will be discussed, except liquefaction, because it is not within the scope of this study.

2.1 Pyrolysis

Pyrolysis is the first step in a combustion or gasification process and literally means the breaking down of a material by heat. It is a devolatilization process in the absence of an oxidizing agent (for example oxigen). After drying the process can be divided into three stages: (1) pre-pyrolysis, between 120 °C and 200 °C accompanied with small weight loss; (2) main pyrolysis at temperatures above 200 °C, with solid decomposition and significant weight loss; (3) continuous char devolatilization, during which resulting C-H and C-O bonds are broken and a small weight loss is noted. [5]

Products of this thermal decomposition process are char (solid), tar (liquid) and volatiles (gas). Gasses released during pyrolysis are usually gasses of low molecular weight. Tars are usually in the vapour phase when extracted from the sample, but can quickly liquidify at temperatures below 450 °C, resulting in a viscous black matter that sticks everywhere and messes everything up. Therefore, during the gasification process, tar is an unwanted product. Char is a carbon rich solid (think of charcoal), that is left after pyrolysis. Depending on the process parameters, different amounts of volatiles can remain inside the char. After complete pyrolysis, no volatiles are left inside the char, only fixed carbon remains. [2]

Tar

Main tar compounds are levoglucosan, furan derivatives and phenols. When looking at the structure of the main components of biomass, cellulose, hemicellulose and lignin (section 1.2) it can be understood where tars come from. One type of tar is levoglucosan (Figure 2.1), which can originate from cellulose or hemicellulose. [6] Furthermore, furan derivatives are possible tar compounds, the furan ring structure has been visualised in Figure 2.2. Other types of tars mainly come from lignin, the only wood component with aromatic compounds. The ring of 6 carbons with alternating single and double bound (benzene ring) is strong and reduces less easy to smaller molecules as for example the rings present in cellulose. Therefore many tar components originate from the wood compound lignin. Faix, Meier and Fortmann, [7] have separated and identified 82 of the thermal degradation products of lignin that were originated during pyrolysis at 450 °C by using gas chromatography followed by mass spectrometry. Almost all identified species are aromatic and many also phenolic (a hydroxyl, OH-, group, connected to an aromatic hydrocarbon group, Figure 2.3).

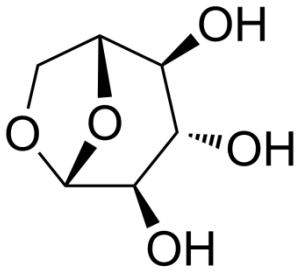

FIGURE 2.1 LEVOGLUCOSAN [8]

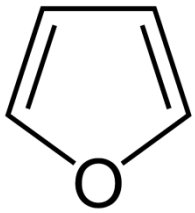

FIGURE 2.2 FURAN RING [8]

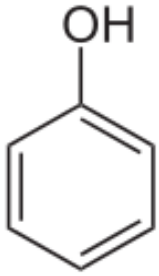

FIGURE 2.3 PHENOL [8]

2.2 Combustion

Ideally, combustion is the complete oxidation (reaction with an oxidizing agent, for example oxygen) of a sample. At molecular level many complicated reactions take place in the gas phase, but the global reaction of total biomass combustion can be expressed as: [2]

$$CH_{1.4}O_{0.6} + 1.05\ O_2 \rightarrow CO_2 + 0.7\ H_2O$$

Or more general [4]:

$$C_xH_yO_z + \left(\frac{y}{4} + x - \frac{z}{2}\right) O_2 \rightarrow xCO_2 + \frac{y}{2}H_2O$$

After drying, the process of combustion can be divided into two stages. At moderate temperatures volatiles are released from the sample and burn and at higher temperatures oxidation of char occurs. [9]

When complete combustion takes place, only fully oxidized products will remain. During a real, not complete, combustion process the following products are formed: water (H_2O), carbon dioxide (CO_2), carbon monoxide (CO) and methane (CH_4), among others. [10]

2.3 Gasification

Essentially, gasification is a partial oxidation process that converts a solid fuel into a gaseous fuel. [2] Except for the drying phase, the process is divided into two stages: devolatilization (temperature range around 200-600 °C); gasification of the remaining char. With raising temperature, volatiles in the material are released, independent of the (oxidizing) agent present. The reactions occurring afterwards, in the vapour phase, depend on the atmosphere. When plenty of oxygen is present, all products will combust and the (main) end components are H_2O and CO_2. When no oxidizing agent is present, big molecules can still change, due to cracking. [11]

During gasification, various products are char, tars, gas, which have already been described in section 2.1. The purpose of gasification for producing (bio-) fuels is the production of a gas called synthesis gas (syngas), which consists of carbon monoxide and hydrogen. [2] Ideally, these two gasses would be the only product and the biomass gasification reaction would be: [4]

$$C_xH_yO_z + (x - z)CO_2 \rightarrow (2x - z)CO + \left(\frac{y}{2}\right) H_2$$

Substitution of the general composition of biomass results in:

$$CH_{1.4}O_{0.6} + 0.4CO_2 \rightarrow 1.4CO + 0.7H_2$$

In a real gasification process not only CO and H_2 will be formed, but the gas product will consist of: carbon dioxide (CO_2), carbon monoxide (CO), hydrogen (H_2), water/steam (H_2O) and methane (CH_4), among others. [5] Whatever remains after complete gasification is the ash. For a simple picture of the gasification process, see Figure 2.4.

Syngas can be used for the production of electricity, fuels and chemicals. The final goal of the GasBio project is to (gain insight in how to) produce a syngas that can be formed into (bio) fuels via the

Fischer-Tropsch method. Therefore this method will be described briefly and various parameters influencing the gasification process will be discussed.

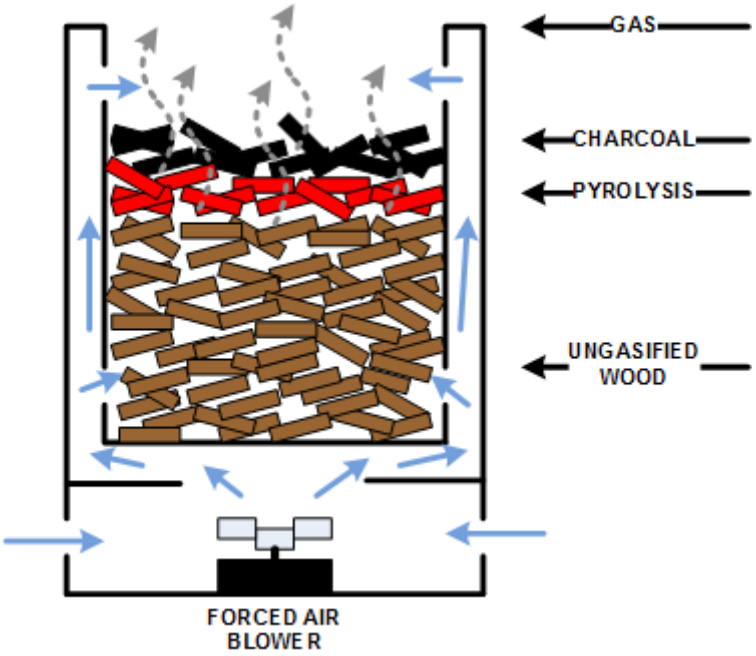

FIGURE 2.4 GASIFICATION PROCESS, ORIGINAL PICTURE FROM: [12]

2.3.1 Fischer-Tropsch synthesis

In Fischer-Tropsch (FT) synthesis, syngas is converted over metal catalysts into aliphatic (non-aromatic) hydrocarbons. Franz Fischer and Hans Tropsch discovered this application in 1923 [13] and basically, via Fischer-Tropsch synthesis the syngas produced by gasification of biomass can be converted into a liquid fuel. This process is not commercial yet for biomass gasification, while it is already for fossil fuels (coal, natural gas). According to Van der Laan [13], the total process can be divided into three stages: syngas production and gas cleaning; Fischer-Tropsch synthesis; product grade up. The Fischer-Tropsch synthesis is nowadays performed over iron or cobalt catalysts in temperature ranges of 200-300 °C and pressures between 10 and 60 bar. [13]

Multiple reactions play a role in the synthesis to aliphatic hydrocarbons. Over an iron catalyst (which is most relevant for bio-syngas) the FT synthesis reaction can be simplified to: [13]

$$CO + \left(1 + \frac{m}{2n}\right) H_2 \rightarrow \frac{1}{n} C_n H_m + H_2 O$$

Different companies are able to make fuels from a syngas via the Fischer-Tropsch method, all using different catalysts. The applicable hydrogen-carbon monoxide (H_2/CO) ratios of the syngas vary per company (per catalyst used) and can be between 1.3 and 2.6. [14] On average it is said that a H_2/CO ratio around 2 is desirable to make it useful for conversion into fuel via Fischer-Tropsch.

2.3.2 Parameters of gasification

As expected, there are many parameters which have an influence on the gasification process. Gasification temperature, residence time, gasifying agent and biomass source will be discussed below.

Temperature

The gasification temperature influences the speed of forming matter, at higher temperatures reactions happen faster. And at different temperatures, different reactions are active. For example the so called water-gas shift reaction, $CO + H_2O \leftrightarrow H_2 + CO_2$, can dominate in the temperature region 500-600 °C and the so called water gas reaction, $C + H_2O \leftrightarrow CO + H_2$, becomes significant at temperatures around 1000-1100 °C and higher. [15] Furthermore, tar cracking, the breaking down of (unwanted) tars into smaller molecules, occurs at temperatures above 600 °C. [15] So the final gas composition and amount of tars varies with reaction temperature.

Residence time

If the residence time of a sample (particle) in the gasifier is too short, the process of gasification will not be finished, because there is not enough time for the reactions to reach equilibrium. Unreacted material will still be present when residence time is too short and ideal gas yield (as much conversion to H_2 and CO as possible) is not reached.

Sample moisture content

Moisture, contained in the biomass sample has to evaporate, which uses energy and reduces the temperature in the gasifier. The use of as little energy as possible and, as discussed above, a higher temperature in the gasifier are desirable. So a low moisture content of the biomass is desirable. [2]

Sample volatile matter

The volatile matter content is directly related to the feedstock reactivity, the speed at which the fuel is converted into gas and higher volatile content results in higher fuel conversion. So biomass, on average containing more volatile matter, is more reactive than carbon-coke (solid residue derived from coal). [16]

Gasifying agent

The gasifying agent is the gas that fills the atmosphere around the biomass particles during gasification. Applicable gasifying agents are for example: carbon dioxide (CO_2), steam (H_2O), pure oxygen (O_2), air (78.1 % N2, 20.9 % O2, 1.0 % others) or mixtures of these.

The use of a different gasifying agent results in a different reactivity and product gas composition. Oxygen is for example much more reactive then steam or CO_2 and gasification with steam is mostly used to produce a hydrogen rich gas. Finally, when an inert gas is present in the gasifying agent, like nitrogen in air, it will also be present in the product gas and has to be removed, which can be expensive. [17], [18]

Others

Other parameters influencing the gasification process are pressure and ratio of gasifying agent and biomass. These parameters are not within the scope of this study, so their influence is not discussed.

3 Analyzing equipment

The equipment used for analyses during the experiments performed in this study are a thermo gravimetric analyzer (TGA), a Fourier transform infrared radiation (FTIR) analyzer and a mass spectrometer (MS). Finally, the total setup is described and the reproducibility of the data is discussed.

3.1 Thermo gravimetric analyzer (TGA)

Generally, a thermo gravimetric analyzer (TGA) measures the mass (-loss or -gain) of a sample subjected to a specified temperature program.

The TGA used is a Q5000 IR, produced by TA Instruments. The Q5000 IR consists of a thermobalance, a furnace and an autosampler. The thermobalance is kept at a constant temperature of 40.00 °C in a chamber that is insulated and purged with gas, usually nitrogen. At the end of the horizontal balance arm, there is the “hang-down wire” ending in a hook, at which the crucible (also called sample holder or sample pan) can be placed. According to TA Instruments the weighting accuracy of the balance is +/- 0.1 % and the weighting precision +/- 0.01 %. [19] The accuracy is the error made by the balance, difference between the measured weight and the real weight, in other words the ability of the balance to show the real weight of the sample. The precision concerns the reproducibility of the measurement, the ability of the balance to show the same mass for the same sample in every measurement.

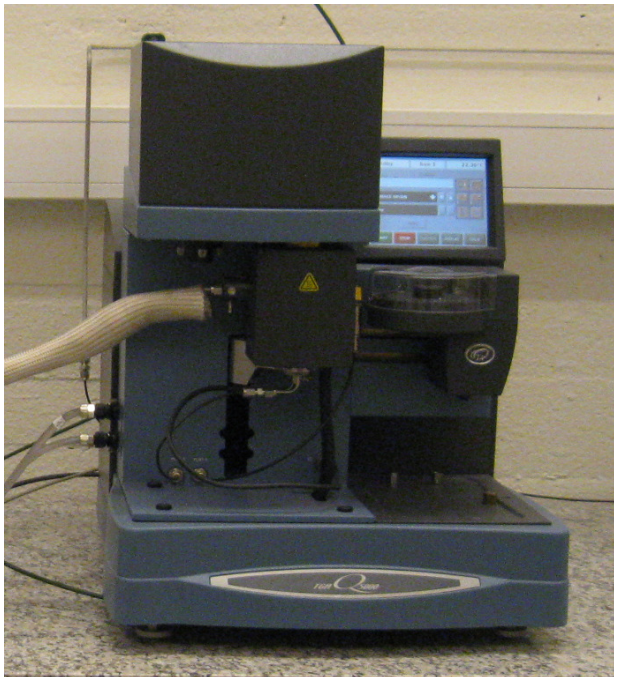

FIGURE 3.1 OVERVIEW PICTURE OF THE TGA (FURNACE IS CLOSED)

FIGURE 3.2 HOOK WITH SAMPLE PAN (CRUCIBLE) ABOVE THE FURNACE [19]

The crucible hangs inside the furnace, which is radiantly heated by infra red lamps outside the furnace chamber. This allows very high heating rates compared to more traditional TGA’s. Furthermore there are less temperature gradients present, which result in uniform heating of the sample, reduced weight error due to convection and more precise and reproducible temperatures. The furnace is insulated by multiple heat shields and a reflector to not influence the measuring equipment by the high temperatures in the furnace chamber. The applicable range of linear heating

ranges from 0.1 °C/min up to 500 °C/min and with a ballistic heating rate the maximum is >2000 °C/min within the temperature range of ambient until 1200 °C. The temperature is measured by a thermocouple with an isothermal temperature accuracy of +/- 1 °C. [19], [20]

The main results obtained from a TGA analysis are the so called TG and DTG graph. The TG graph shows the weight (percentage) as a function of time (or temperature) and the DTG graph shows the first derivative of the TG curve. Often these graphs are combined in one picture. An example of such a picture can be seen in Figure 3.3.

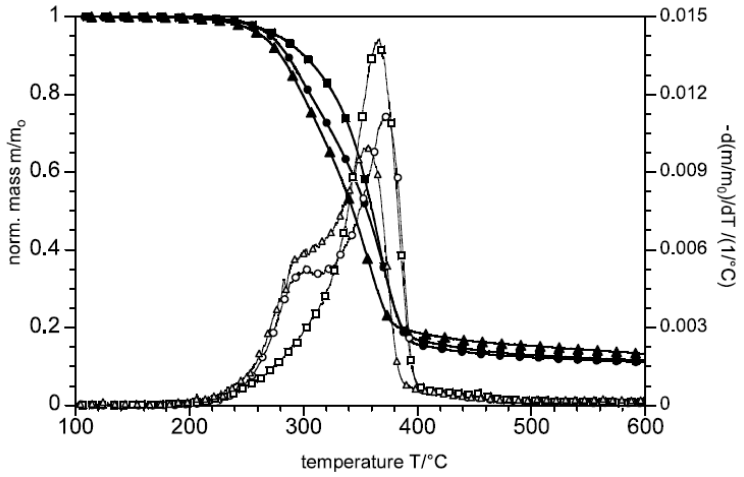

FIGURE 3.3 TG AND DTG CURVES OF CHEMICALLY TREATED HORNBEAM WOOD: HEATING RATE B=10 °C MIN-1. BOLD LINES AND FILLED SYMBOLS REPRESENT TG CURVES, THIN LINES AND OPEN SYMBOLS REPRESENT DTG CURVES. -▲-, UNTREATED; -●-, WATER WASHED; -■-, ACID WASHED. [6]

As explained in section 1.2, wood mainly consists of cellulose, hemicelluloses and lignin. These three components have been separately heated under nitrogen atmosphere by Cagnon *et al.* [21], Figure 3.4, and showed to have different reactivity. It is known that wood reacts in superposition of these components. Hemicellulose is the "most reactive" of the three, in other words, it reacts at the lowest temperatures (except from the drying just above 100 °C). Cellulose is the second most reactive and lignin reacts over a larger temperature region, but has the main weight loss at higher temperatures, the little slope above 400 °C in Figure 3.3 is therefore caused by the reaction of lignin.

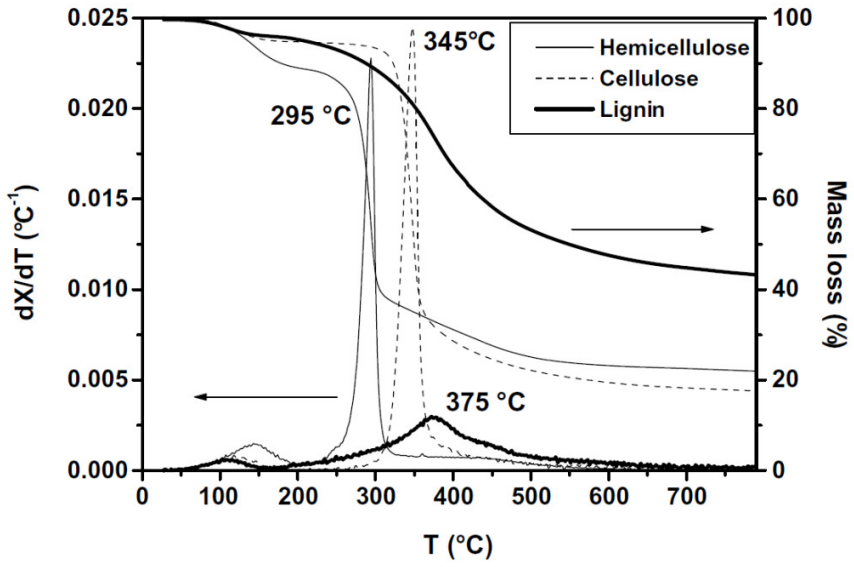

FIGURE 3.4 HEMICELLULOSE, CELLULOSE AND LIGNIN TG-DTG EXPERIMENTAL CURVES AT 10 °C MIN^{-1} UNDER NITROGEN. [21]

Sun *et al.* have modelled the decomposition of the three main wood components and compared the sum of the three separate models to experimental results, Figure 3.5. [22]

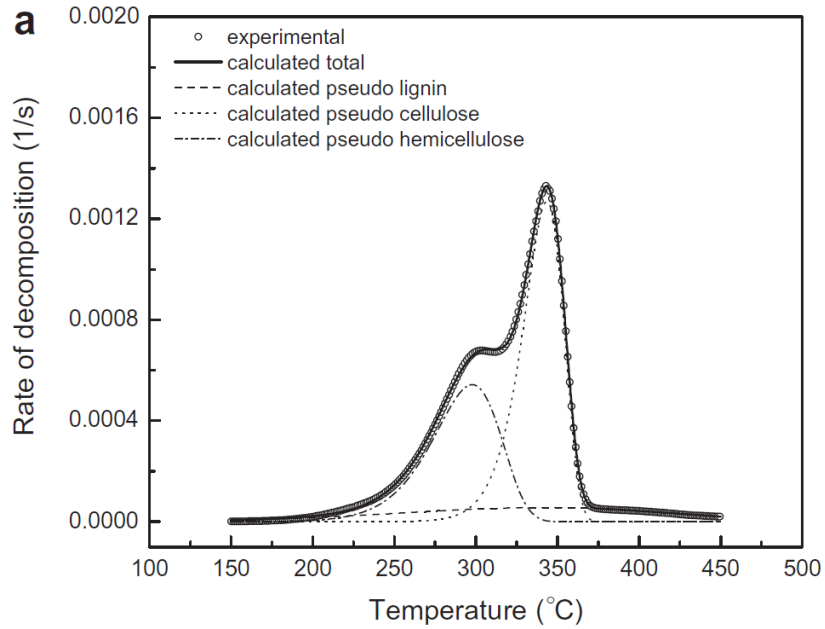

FIGURE 3.5 DECOMPOSITION INTO HEMICELLULOSE, CELLULOSE, LIGNIN AND THERE SUM [22]

When a wood type contains more hemicellulose, the so called hemicellulose-shoulder (around 300 °C) will be more visible. Typically hardwoods contain more hemicelluloses then softwoods. In Figure 3.3 the hemicelluloses shoulder is visible for the untreated and water washed hornbeam, but not for the acid washed hornbeam due to the removal of hemicelluloses by acids. [2], [6]

3.2 Fourier transform infrared radiation (FTIR) analyzer

In this study a Fourier transform infrared radiation (FTIR) analyzer, using infrared spectroscopy, was used to analyze the gasses evolving during the experiments. In this context the word “sample” corresponds to the evolved gasses which are led through the FTIR analyzer. The FTIR used in these experiments is the “Nicolet iS10 FTIR Spectrometer”, produced by Thermo scientific (Figure 3.6). The spectrometer from Thermo Scientific includes a database with many known spectra from various species. With the software, spectra can be analyzed, the database can be searched for matching spectra and accuracy and speed of the measurement can be set. [23]

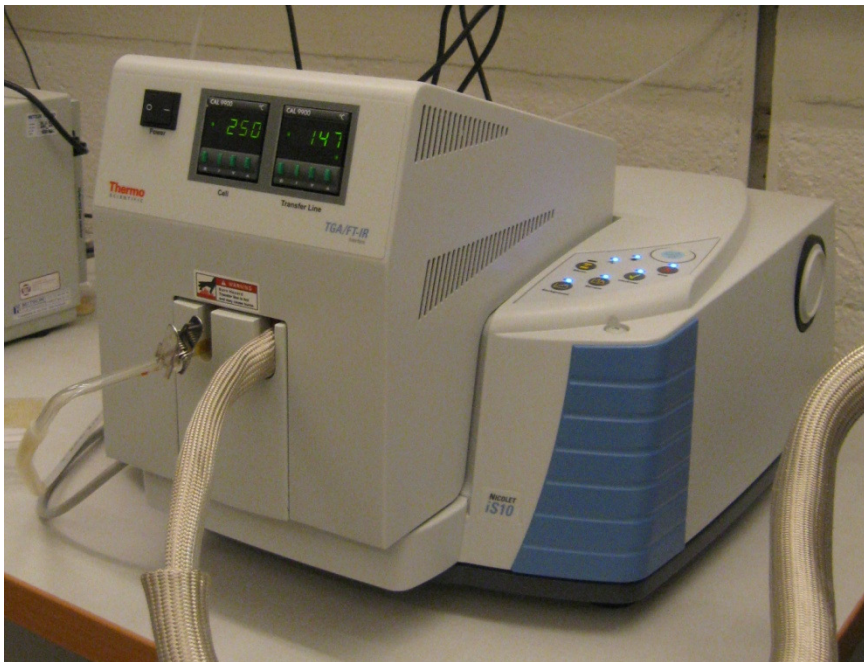

FIGURE 3.6 THERMO SCIENTIFIC, NICOLET IS10 FTIR SPECTROMETER

The FTIR spectrometer contains an optical bench and software. The bench consists of multiple components (Figure 3.7). The infrared source emits the infrared light, which first passes through the interferometer, splitting the beam, sending it to a fixed and a moving mirror and recombines both beams. This causes the intensity of the recombined beam to change constantly and this change is different for each measured frequency. A laser beam, with an exact known frequency, follows the same path as the IR beam, so the exact location of the moving mirror can be determined. After the beam has been encoded by the interferometer, it passes through the sample, which in this case is the gas cell through which the exhaust gasses from the TGA are led. The sample absorbs energy from various wavelengths and therefore alters the beam, for example the C=O stretch absorbs energy near 1750 cm^{-1}. [24] Subsequently, the detector measures the intensity of the beam, which results in an interferogram, a graph showing the amount of infrared radiation reaching the detector. [24]

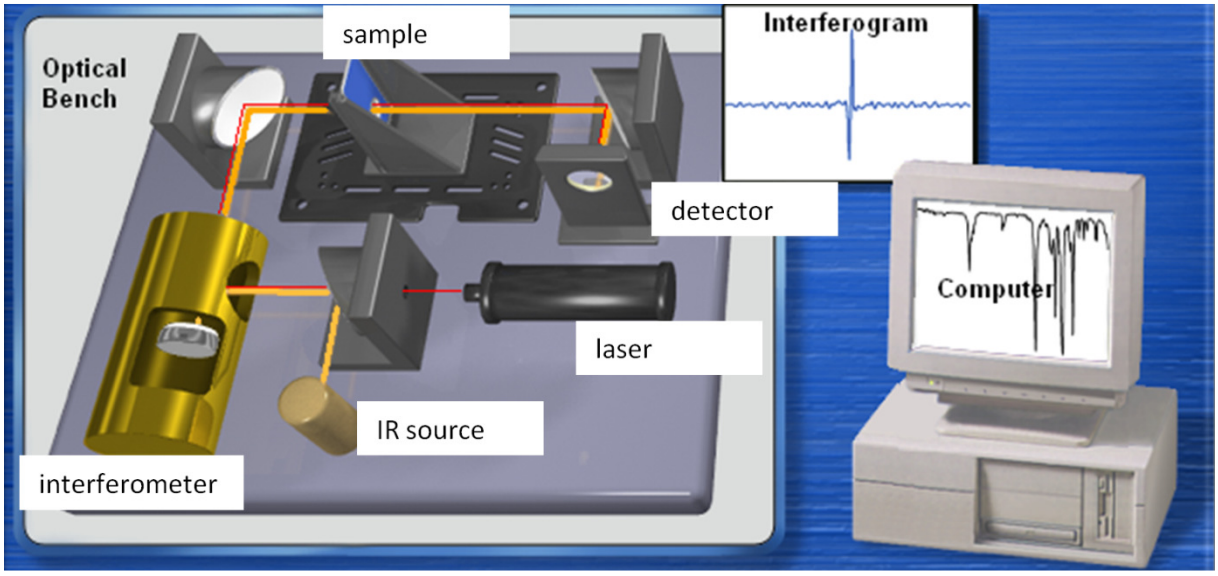

FIGURE 3.7 OPTICAL BENCH FTIR [24]

By taking a background before inserting the sample, the interferogram of the components of the optical bench is taken. Fast Fourier transform is used to calculate the intensity of the beam for each frequency from the interferogram, the result is called a single beam spectrum or single beam energy curve. This transformation is done both for the background spectrum and for the sample spectrum (or spectra). The sample single beam spectrum is divided by the background single beam spectrum, resulting in a transmittance spectrum solely caused by absorption of energy by the sample and without influence of the internal components of the optical bench. In a transmittance spectrum the transmittance through the sample is shown, which can also be converted to absorbance (showing the amount of radiation absorbed by the sample). Both absorbance and transmittance are usually shown as a function of the wave number [cm^{-1}], the number of waves that fit into 1 cm. [24]

Multiple scans can be performed and are averaged for one final spectrum, resulting in an increased signal to noise ratio and increased sensitivity of the instrument. Furthermore, resolution and data point spacing are related. To identify two separate peaks in a spectrum three data points are needed two for both peaks and one between the peaks. So to be able to identity two peaks that are 8 cm^{-1} apart, a resolution of 8 cm^{-1} is needed, corresponding to a data point spacing of 4 cm^{-1}. [24] The combination of these settings (number of spectra averaged and resolution) results in a measurement time, accuracy and precision of the resulting spectrum. Preferable results would combine high accuracy and short measurement times, to detect evolved gasses right away. Because the experiment time at high heating rates is relatively short, this is expected to be a challenge and a balance between parameters has to be found.

Furthermore, the FTIR is incapable of detecting symmetrical compounds, like N_2 or H_2. As hydrogen is one of the main components of the syngas produced during gasification, this is drawback of the FTIR.

As an example, a spectrum of carbon dioxide retrieved from the Omnic library [24] is shown in Figure 3.8. Carbon dioxide absorbs wavelengths in three regions, with different intensity. Most of the absorption takes place between 2300 and 2390 cm^{-1}, where two characteristic CO_2 peaks appear. Smaller absorption takes place around 670 cm^{-1} and between 3570 and 3760 cm^{-1}, where one and four peaks occur, respectively.

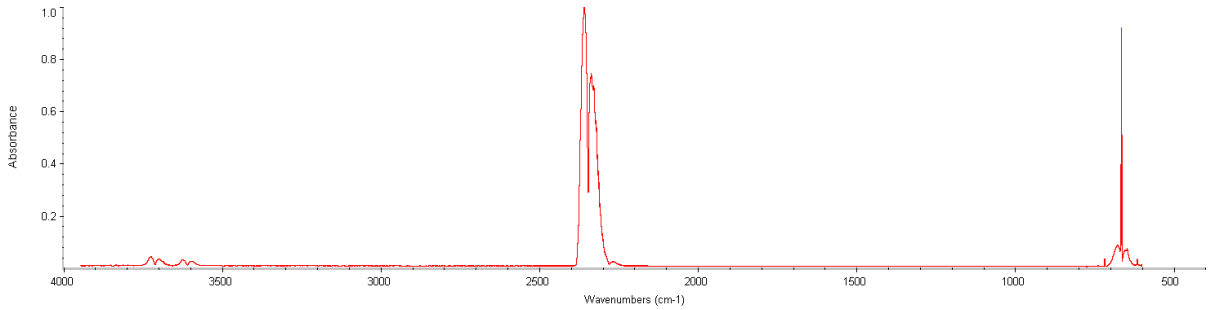

FIGURE 3.8 FTIR SPECTRUM CO_2 [24]

3.3 Mass spectrometer

Generally, a mass spectrometer (MS) consists of an ion-source, a mass filter and a detector, Figure 3.9. The MS used in this study is a ThermoStar^{TM} GSD 301 T300 from Pfeiffer Vacuum, Figure 3.10.

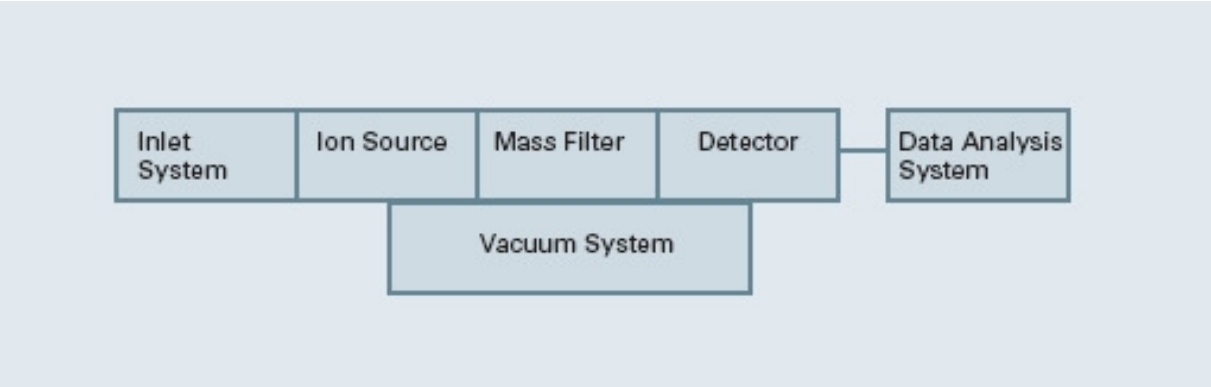

FIGURE 3.9 COMPONENTS OF A MASS SPECTROMETER [25]

The sample, which is in this case the exhaust gasses from the TGA, is let in to the MS via a capillary and partially pumped down to the working pressure. In the ion source, the sample is bombarded with ions, producing singly and multiply charged positive molecular ions and positively charged fragmented ions. In a mass filter, the created ions are separated on their mass to charge ratio. The mass filter used in this MS is a quadrupole, consisting of four parallel rods arranged in a square, which let, depending on the voltages applied to the rods, a particle with a certain mass to charge ratio go through, while others collide with the rods. In this way, the ions are separated on their mass to charge (m/z) ratio and only one ratio or one region of ratios can reach the detector. The MS used has two detectors, a Faraday detector and a C-SEM (continuous secondary electron multiplier) detector. Simplified, both register ions striking the detector and measure the voltage generated by these hits. The C-SEM detector is used in all experiments performed in this study, because it has a higher sensitivity, so lower amounts can be measured in shorter times and the signal to noise ratio is higher. [25]

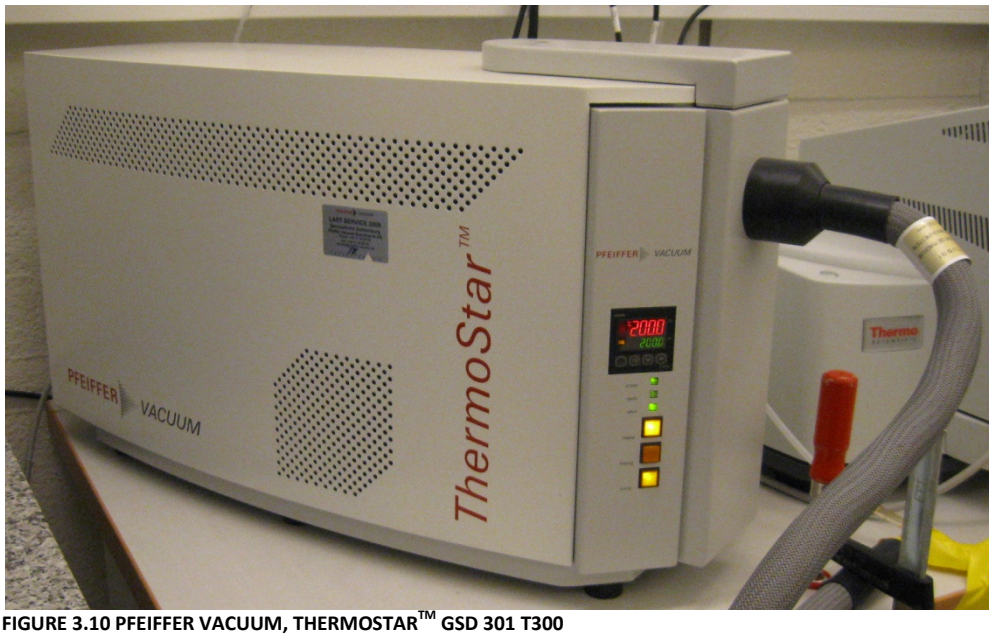

FIGURE 3.10 PFEIFFER VACUUM, THERMOSTAR™ GSD 301 T300

A disadvantage of the C-SEM detector is that the amplification factor can change over time [25] and therefore the intensity of two masses in two experiments can only be compared globally. Furthermore, the instrument is not calibrated for the detected mass to charge ratios; therefore the

intensities of two peaks of different m/z ratios cannot be compared. This is the reason that in this study, only semi-quantitative results are obtained from MS data.

Each molecule has a certain probability to split into certain fragments when bombed with electrons, the so called fragment distribution. If, for example, specimen ABC is led into the MS for detection, after bombarding it with ions, molecular ions or various fragment ions can be formed. For example: - $ABC + e^- \rightarrow ABC^+ + 2e^-$ (a singly charged molecular ion), or $ABC + e^- \rightarrow AB^+ + C + 2e^-$ (a fragment ion). Each fragment ion has a certain probability to originate during electron bombardment. From the combination of the different mass to charge ratios (for example from ABC^+ and AB^+) the original specimen can be discovered. As a numerical example, the fragment distribution of carbon dioxide, with mass of 44 amu (atomic mass unit) is presented in Table 3.1. [25]

TABLE 3.1 CARBON DIOXIDE FRAGMENT DISTRIBUTION [25]

m/z ratio	%
44	100
28	11
16	9
12	6

As a consequence of this specific distribution, the peak height of m/z ratio 28 will be 11 % of the peak height of m/z ratio 44 for the compound CO_2. When different compounds are detected in one sample, their contributions will add up.

3.4 Setup description

The individual components described above are combined in the total set-up, Figure 3.11. During the experiments evolved gasses are swept away by a sample purge flow of 50 ml/min. For pyrolysis experiments nitrogen (N_2) is used as an inert gas, for combustion synthetic air (80 % N_2, 20 % O_2) is used and for gasification experiments carbon dioxide (CO_2) is diluted with nitrogen by mass flow controllers connected to a gas mixing chamber, Figure 3.12 (25 ml/min CO_2; 25 ml/min N_2). Furthermore, the balance is purged with 20ml/min N_2, to keep the balance room pressurised and prevent possible corrosive gasses entering the room containing the delicate balance. All used gasses are delivered by Yara Praxair and have a purity of 5.0 (99.999 %).

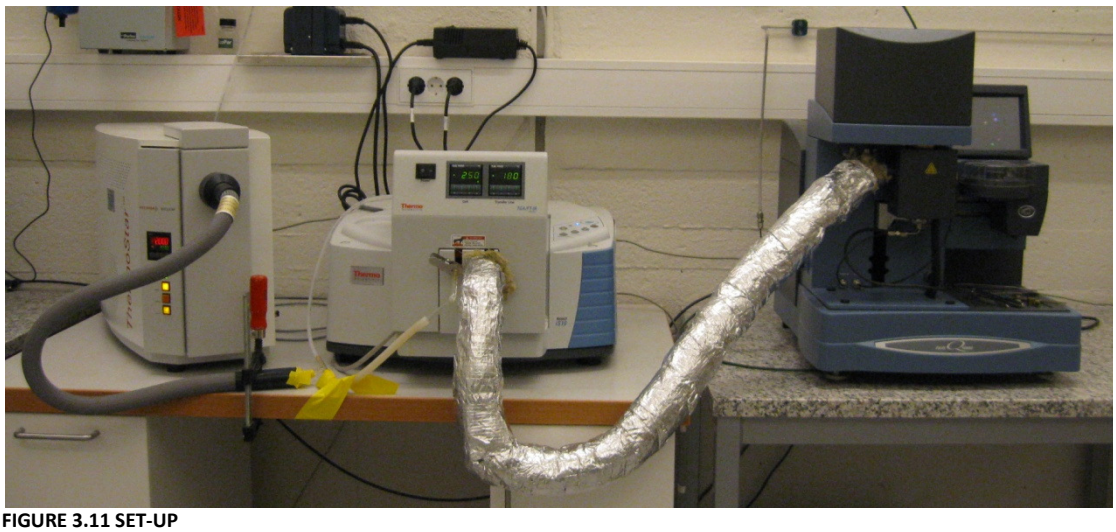

FIGURE 3.11 SET-UP

All gasses (sample purge flow, balance purge flow and evolved gasses) are led through the insulated and heated transfer line to the FTIR and into the FTIR gas cell, where the composition of the gasses is detected by infra red radiation analysis. The gas cell is heated to a temperature of 250 °C and the transfer line is heated to 180 °C. The temperature of the transfer line is lower then the gas cell to make sure that condensation of product gas will occur in the transfer line and not inside the gas cell, since the transfer line is easier to clean.

By using a relatively high flow rate the produced gasses are swept away almost immediately from the sample out of the hot furnace chamber into the cooler transfer line to prevent them from reacting further.

Next to the FTIR, the MS is connected and all gasses are led into a non-heated transfer line in which the capillary of the MS is positioned. A fraction of the gasses is led through the capillary into the MS for detection and the remaining gasses are led into the ventilation.

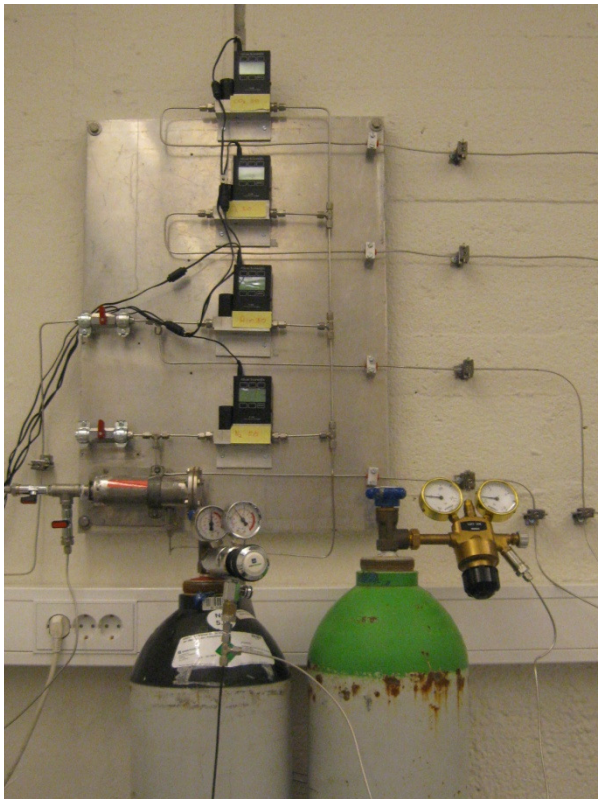

FIGURE 3.12 GAS MIXING

During experiments first the weight of the crucible is tared to a maximum weight of 0.01 mg. Approximately 4-5 mg sample is put on the crucible inside a microbalance and the crucible is loaded on the hook by the auto sampler. The furnace is closed and the chambers and lines are purged with the correct gasses for at least 30 minutes to create the right atmosphere. After 30 minutes, the background for the FTIR is taken, after which the FTIR goes into the time out status, until it receives an external trigger from the TGA at the start of the experiment. Next, the MS is started manually and subsequently the TGA. At the moment the experiment starts (when the TGA gives the external trigger to the FTIR) the time the MS is ahead of the TGA is noted.

3.5 TGA blank subtraction

To see the influence of temperature on weight changes of the (empty) crucible, blank preliminary experiments were performed. Two methods with low and high heating rate were used. In the first method the sample flow (10 ml/min N_2) was purged for 15 minutes, after which the temperature was raised up to 900°C with a heating rate of 50°C/min. For the method 2 the same purging time was used; the furnace chamber was heated up to 900°C at a heating rate of 500°C/min and kept at 900°C for 10 minutes. Results for the blank experiments and experiments with sample (spruce) for both applied methods can be seen in the figures below.

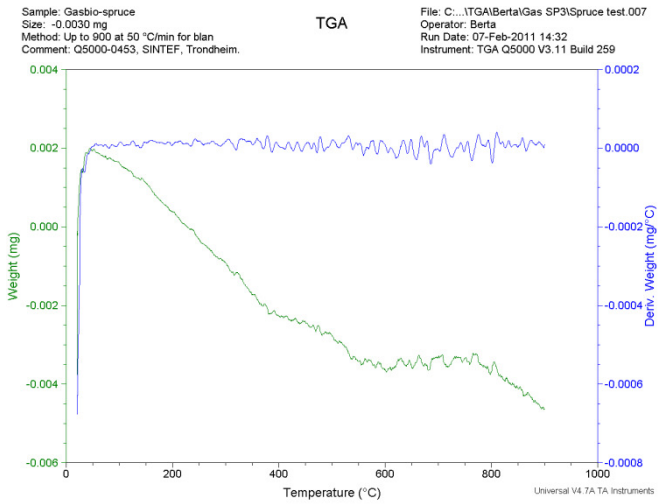

FIGURE 3.13 BLANK, METHOD 1

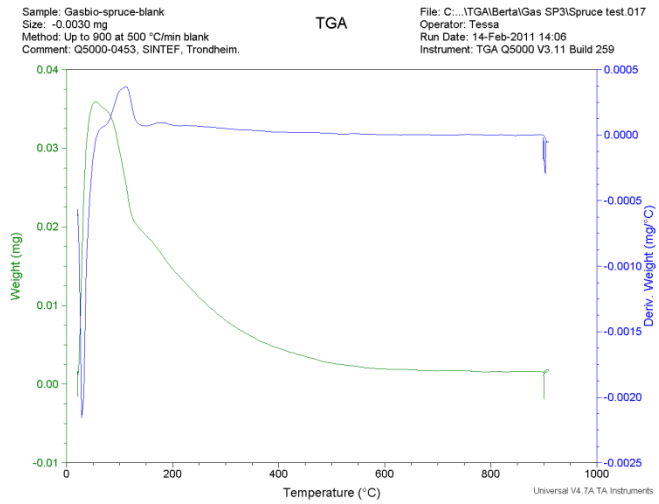

FIGURE 3.14 BLANK, METHOD 2

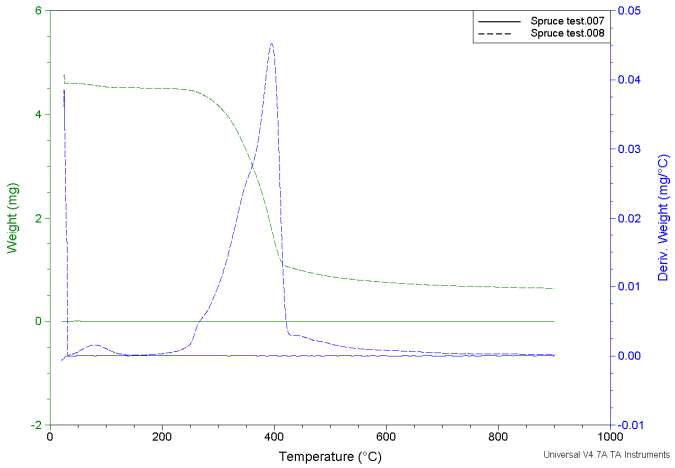

FIGURE 3.15 SPRUCE PYROLYSIS (DASHED LINE) AND BLANK (SOLID LINE), METHOD 1

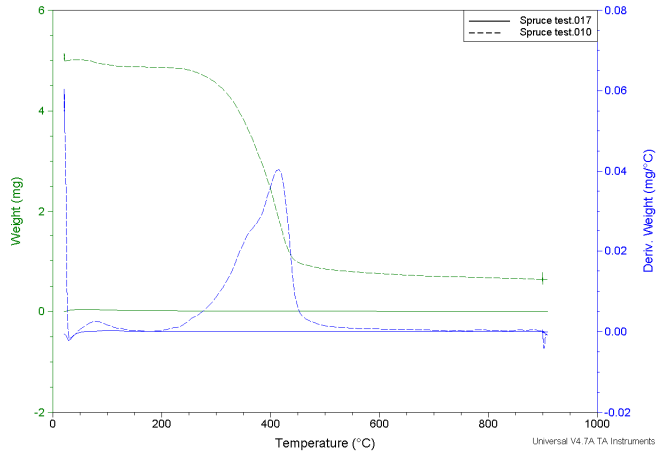

FIGURE 3.16 SPRUCE PYROLYSIS (DASHED LINE) AND BLANK (SOLID LINE), METHOD 2

As can be seen from Figure 3.13 and Figure 3.14, the changes in weight of the empty crucible are for both slow and high heating rates very limited. In numbers the noted weight changes of the empty crucible for method 1 (50 °C/min) are between -4 µg and +2 µg. For method 2 (500 °C/min) the maximal weight changes where between -1.4 µg en +36 µg.

It can be concluded that weight changes of the empty crucible are larger at higher heating rates. The main weight changes of the crucible occur in the lower temperature region. Above 200 °C still a

maximum change of +15 µg was observed, which is slightly higher than the baseline flatness smaller than 10 µg, as claimed by Els Verdonck, application support, TA Instruments.

If the weight changes of the empty crucible are compared to the weight changes of crucible with sample (Figure 3.15 and Figure 3.16) the flatness of the baseline can be observed. The weight changes that occurred during the blank experiments are considered small enough in order to neglect the baseline during the rest of the experiments.

3.6 Reproducibility

To check the consistency of the produced data during the experiments the reproducibility of the experiments has been examined. At the beginning and the end of all experiments the same experiment, spruce combustion at 50 °C/min, has been performed twice on different days.

All data, from TGA, MS and TFIR, has been compared for the four reproduced experiments and will be discussed below.

3.6.1 Reproducibility TGA data

TG and DTG graphs from the four runs of spruce combustion at 50 °C/min have been plotted in Figure 3.17. In this section, only the reproducibility of the data will be discussed, for further discussion of the data, see section 5.2. The difference in location of the first peak around 370 °C (first stage of combustion), is maximally 2.1 °C and the peak height differs 0.027 %/°C, maximally. Furthermore, the first peak starts and ends at the same temperature for all reproduced experiments. More variation exists in the peak location of the second stage of combustion, around 480 °C. This is due to the presence of ignition in the sample. Ignition is specified as the onset of glowing combustion in the sample and is evident by a precipitous weight loss [26]. This steep weight loss is clearly visible in the TG curve, during the second stage of combustion, Figure 3.18. When (a part of) the sample ignites, it will consume all oxygen in the surrounding, causing the ignition to extinguish due to the lack of oxygen. This process is not reproducible by definition, but what is important is that the second stage of combustion starts and ends at the same temperatures for all experiments (440-530 °C). Only the presence or absence of an ignition shifts the peak location.

Concluding, the changes in peak location and start and end temperatures of weight loss in the TGA data are small enough and the TGA data can be called reproducible.

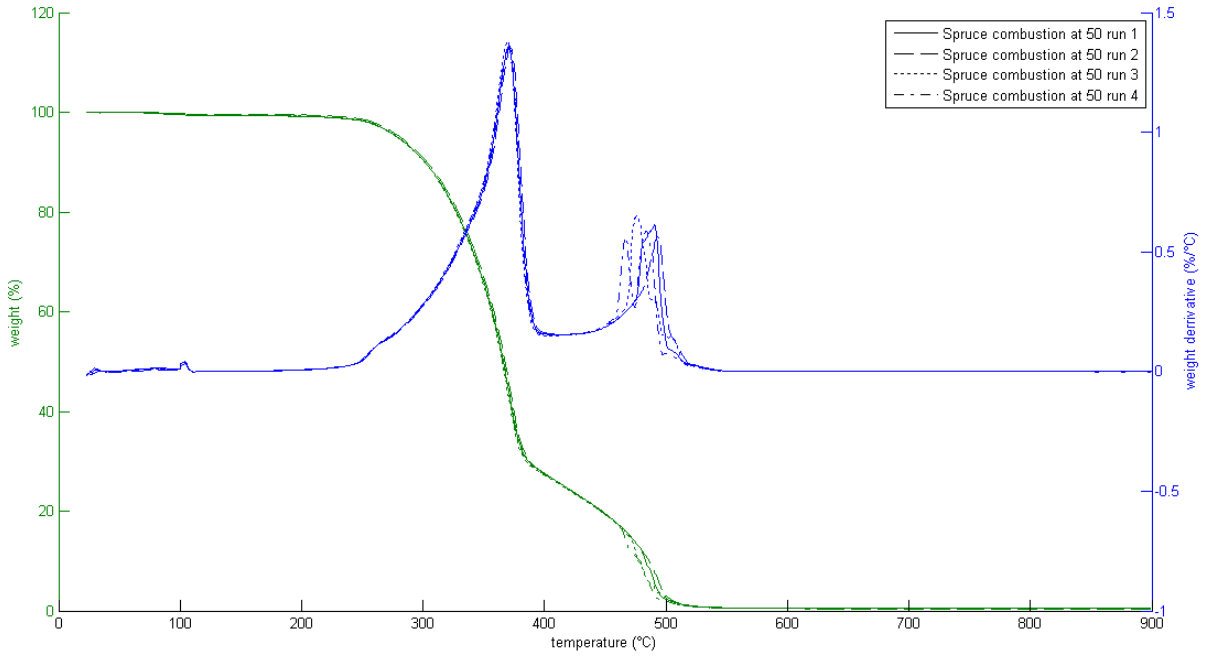

FIGURE 3.17 REPRODUCING TGA

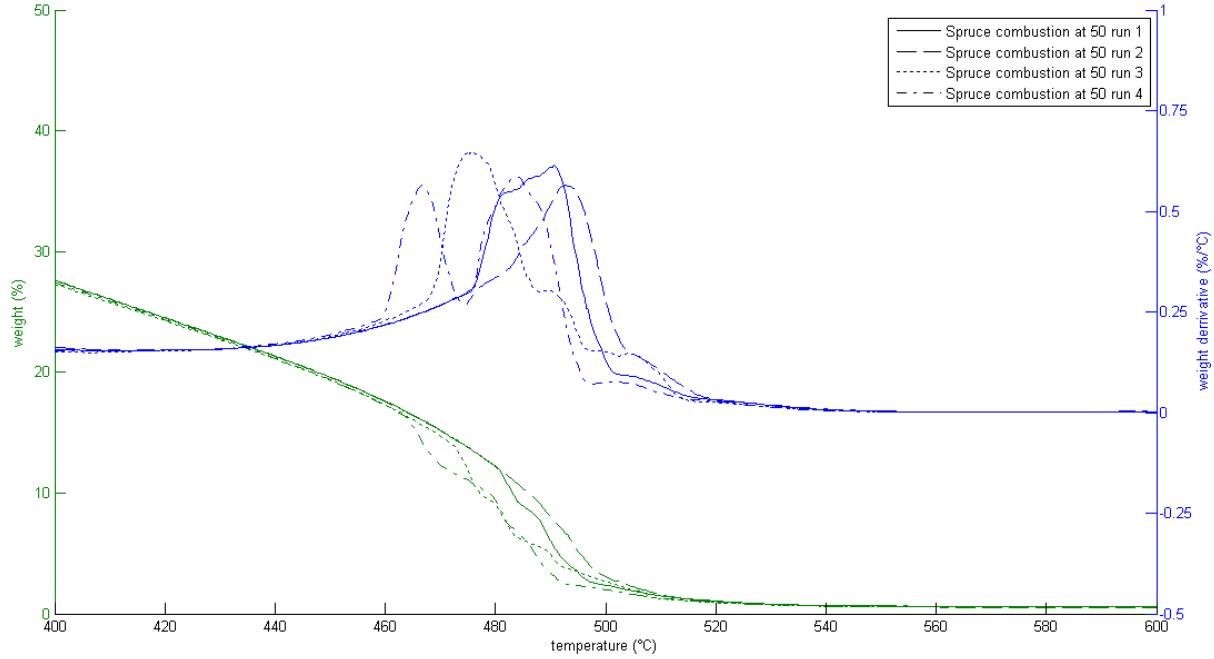

FIGURE 3.18 REPRODUCING TGA, ZOOM

3.6.2 Reproducibility MS data

All detected mass to charge (m/z) ratios have been compared for the reproduced spruce combustion at 50 °C/min experiments. The same group of masses are showing just noise during the combustion experiments, these are mass to charge ratios 2, 15, 16, 26, 27, 60, 94, 96, 108, 118, 124, 126. The masses, which are not showing just noise are mass to charge ratio 18, 30, 32, 44, 46, 58 and 68. They are showing the same profile and have peaks at approximately the same temperatures. Compounds corresponding to these mass to charge ratios are mentioned in Table 4.2. As an example the results from m/z ratio 44 have been plotted in Figure 3.19 for all reproduced combustion experiments. The shift in peaks is similar for all these masses, for example, for run 2 compared to run 1, all peaks are

shifted approximately +6 °C. This implies that the cause of the error lies in an error in the delay time (time the MS is ahead of the TGA at the start of the experiment).

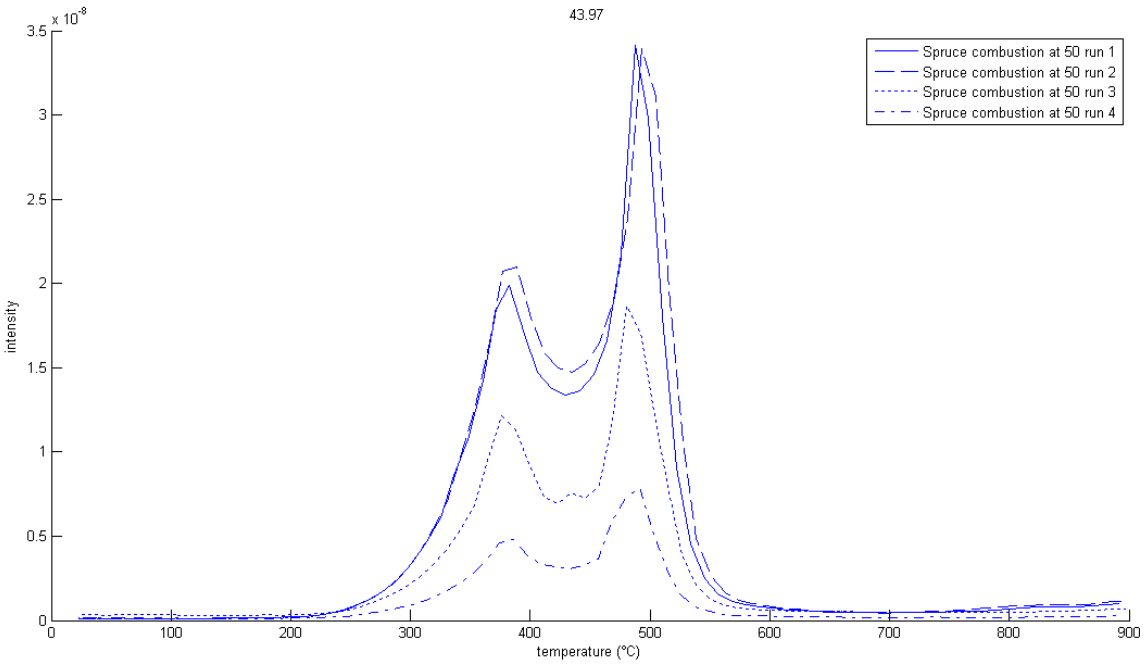

FIGURE 3.19 REPRODUCING MS

The intensity of the data is approximately similar for run 1 and 2, but is considerably lower for run 3 and 4. This can be explained by the amplification factor of the C-SEM detector inside the MS changing over time and emphasizes that intensities of masses during different experiments cannot be compared quantitatively.

Concluding, except the known drawbacks related to the MS, the positions of the peaks in the MS data are reproducible but the magnitude of the peaks is not.

3.6.3 Reproducibility FTIR data

In some experiments, the FTIR has produced reproducible data, like for example in run 1 and 2 of the spruce combustion experiments (Figure 3.20). Unfortunately, especially the behaviour around wave numbers of water and carbon dioxide has been proven to be not reproducible during other experiments. Therefore, some of the good data will be shown and briefly explained here. But the FTIR data should be handled with care. Furthermore, a certain uncertainty, especially in the wave number ranges of water and carbon dioxide should be taken into account.

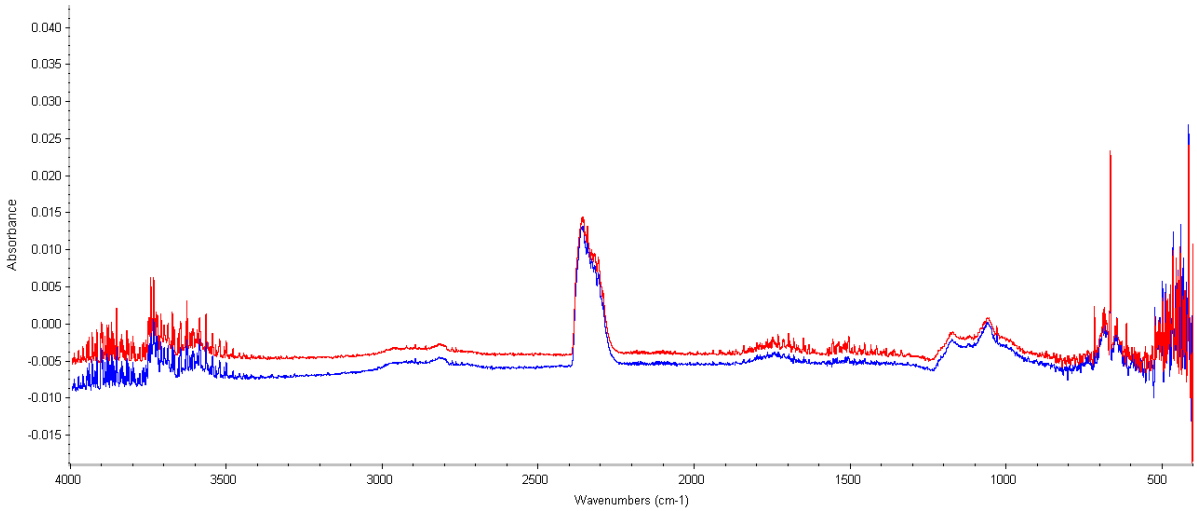

FIGURE 3.20 REPRODUCING SPRUCE COMBUSTION (RED: RUN 1, BLUE: RUN 2)

As an example of some of good data, the 3D picture resulting from the FTIR analysis of spruce pyrolysis at 50 °C/min is shown in Figure 3.21. The maximum absorbance of all wave numbers occurs at 17.5 min after the start of the experiment. The spectrum at this time is shown in Figure 3.22. In this figure the evolution of water, hydrocarbons, carbon dioxide, carbon monoxide, acids and carbonyl groups and carbohydrates, acids and phenols can be seen. [27], [28], [29], [30]

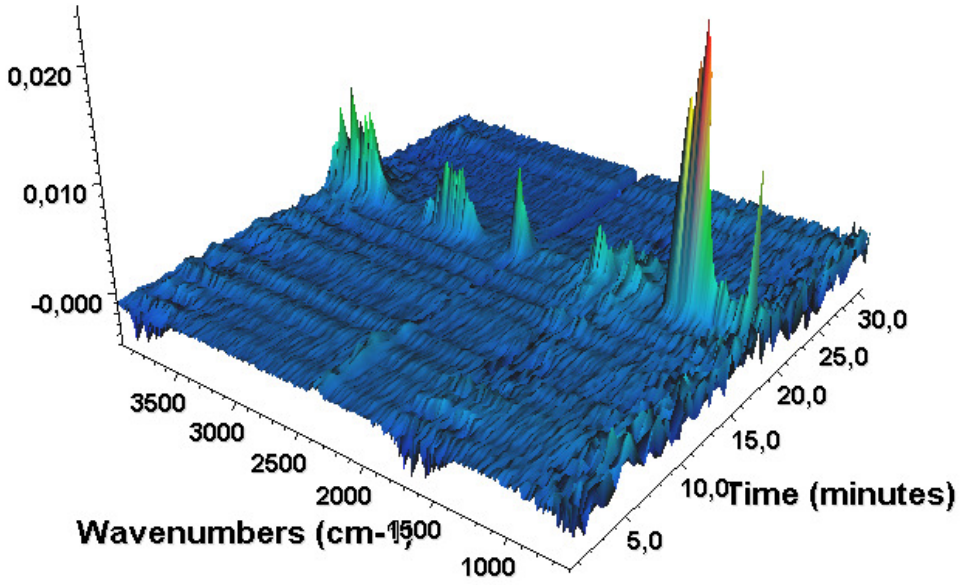

FIGURE 3.21 SPRUCE PYROLYSIS AT 500 °C/MIN (3D)

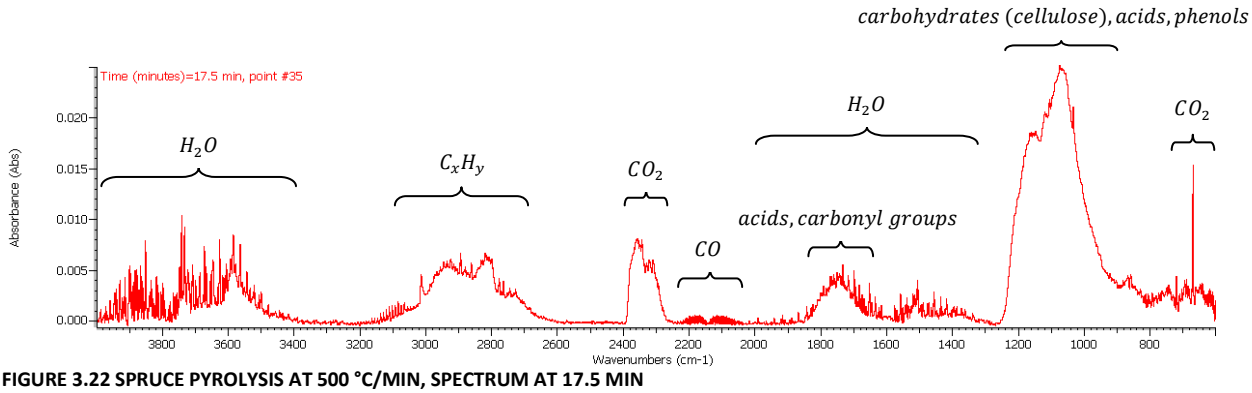

FIGURE 3.22 SPRUCE PYROLYSIS AT 500 °C/MIN, SPECTRUM AT 17.5 MIN

4 Experimental matrix

In Table 4.1, the experimental matrix is given. In all experiments a flow of 50 ml/min is used.

In the experimental table some terms and abbreviations are used. In the feedstock column spruce char-50 corresponds to char produced by pyrolysis at a low heating rate (50 °C/min) and char-500 corresponds to char produced by pyrolysis at a high heating rate (500 °C/min). In the heating rate column a 'g' corresponds to a gradually introduced heating rate, which will be explained in more detail below.

TABLE 4.1 EXPERIMENTAL MATRIX

Process	Feedstock	Heating rate [°C/min]	Isothermal temperature [°C]	Agent [-]
Combustion	Spruce	50	900 (0 min)	Air
Combustion	Spruce	500	900 (0 min)	Air
Pyrolysis	Spruce	50	900 (0 min)	N_2
Pyrolysis	Spruce	500	900 (0 min)	N_2
Combustion	Spruce char-50	50	900 (0 min)	Air
Combustion	Spruce char-500	50	900 (0 min)	Air
Gasification	Spruce char-50	50	900 (30 min)	CO_2; N_2 (1:1)
Gasification	Spruce char-50	500g	900 (30 min)	CO_2; N_2 (1:1)
Gasification	Spruce char-50	500g	800 (60 min)	CO_2; N_2 (1:1)
Gasification	Spruce char-500	50	900 (30 min)	CO_2; N_2 (1:1)
Gasification	Spruce char-500	500g	900 (30 min)	CO_2; N_2 (1:1)
Gasification	Spruce char-500	500g	800 (60 min)	CO_2; N_2 (1:1)
Gasification	Spruce	50	900 (30 min)	CO_2; N_2 (1:1)
Gasification	Spruce	500g	900 (30 min)	CO_2; N_2 (1:1)
Gasification	Spruce	500g	800 (60 min)	CO_2; N_2 (1:1)

All experiments started with a drying phase. The sample has been heated up to 100 °C at a heating rate of 50 °C/min and kept at 100 °C for 15 minutes. Due to some different settings that have been tried, the combustion experiments with a slow heating rate (50 °C/min) dried 10 minutes at 105 °C. At the end of both drying stages the rate of weight loss was both smaller then 0.06 %/°C.

In all combustion and pyrolysis experiments, the sample was, after the drying stage, heated up to 900 °C at the heating rate specified in the experimental matrix. For all samples used in gasification (spruce, char-50, char-500) first gasification at slow heating rate (50 °C/min) and an isothermal stage at 900 °C was applied, to see the start of the weight loss. After that, all samples were gasified at an 'isothermal' temperature (800 or 900 °C) to which they were heated at a gradually introduced heating rate of 500 °C/min. When the heating rate of 500 °/min was used solely, this resulted in a large temperature overshoot. Therefore, the high heating rate was introduced in five steps, with heating rates of 50, 150, 250, 350 and 450 °C/min. Every heating rate step was applied for approximately five seconds. Slowing down of the heating was performed exactly the other way around. By using this heating of 500 °C/min gradually (500g), it takes about 2.0 min instead of 1.7 min, to heat up to 900°C, so this influence is considered negligible and the overshoot in temperature disappeared.

For the FTIR, 16 scans with 2 resolution where used during all experiments, since gas samples normally require a resolution of 2 wave numbers and it is advised to start with averaging 16 scans

[31]. The bench gain was set to 1 and the scanned range was between 600 and 4000 cm^{-1}. Interferograms were stored and a repeat time of 30 s was used, corresponding to 16 scans with 2 resolution.

In the MS, not all masses to charge ratios were scanned, this resulted in a shorter scan time. Mass to charge ratio's 26, 27, 94, 108, 118, 124, 126 were scanned, but showed only noise during all experiments. This is expected to mainly be due to little formation of these compounds and condensation in the transfer lines. Other masses that were scanned and showed more then just noise are shown in Table 4.2.

Carbon monoxide is not mentioned in Table 4.2, because carbon monoxide and nitrogen have the same mass and therefore interfere in the MS data.

TABLE 4.2 SCANNED M/Z RATIOS IN MS, NOT SHOWING JUST NOISE

m/z	**Compound**
2	Hydrogen (and others)
15	CH_3^+, coming from methane/methyl group
16	CH_4^+, coming from methane
18	H_2O
30	Aldehydes, $HCHO^+$ (mainly formaldehyde)
32	Methanol, CH_3OH^+
44	CO_2
46	Organic acids, $HCOOH^+$
58	Propanal
60	Hydroxyl
68	Furan
96	Furfural

Mass spectra are taken continuously after one another. As a result, the relative intensity of one (or multiple) mass to charge ratio(s) can be plotted over time. By accounting for the delay between the TGA and the MS, the corresponding temperature can be looked up, so with a certain error in temperature, intensity-temperature graphs can be presented for each m/z ratio. When comparing MS data with the corresponding TGA data, this error depends on the heating rate and estimated to be 3.3 °C (50 °C/min) and 33 °C (500 °C/min).

5 Results and discussion

In this section influence of applied heating rate on spruce combustion and pyrolysis will be discussed. Furthermore, char gasification, char reactivity and direct gasification will be addressed. Finally the influence of gasification temperature and the influence of gasification in one or two steps will be examined.

5.1 Reactivity definition

In this section, the reactivity of various samples subjected to a thermal degradation process will be mentioned and therefore the word 'reactivity' needs to be well defined. Usually, reactivity is described as the derivative of the mass (M) to time preceded by a certain factor [32], [33], [34]. Therefore reactivity will be defined here as: [32]

$$R = -\frac{1}{M}\frac{\delta M}{\delta t}$$

In words, when a sample starts to react earlier (at lower temperatures) the reactivity of that sample compared to the other one is considered higher. Furthermore, a faster weight loss, corresponding to a higher peak in the DTG curve, is considered to be more reactive than slower weight loss. In other words, the peak height is directly proportional to the reactivity, while the time (or temperature) corresponding to this peak height is inversely proportional to the reactivity. [35]

5.2 Influence of heating rate on spruce combustion

Experiments of spruce combustion have been conducted at heating rates, 50 °C/min and 500 °C/min. The DTG data from these experiments is plotted in Figure 5.1 and the MS data for mass 44 has been plotted in Figure 5.2.

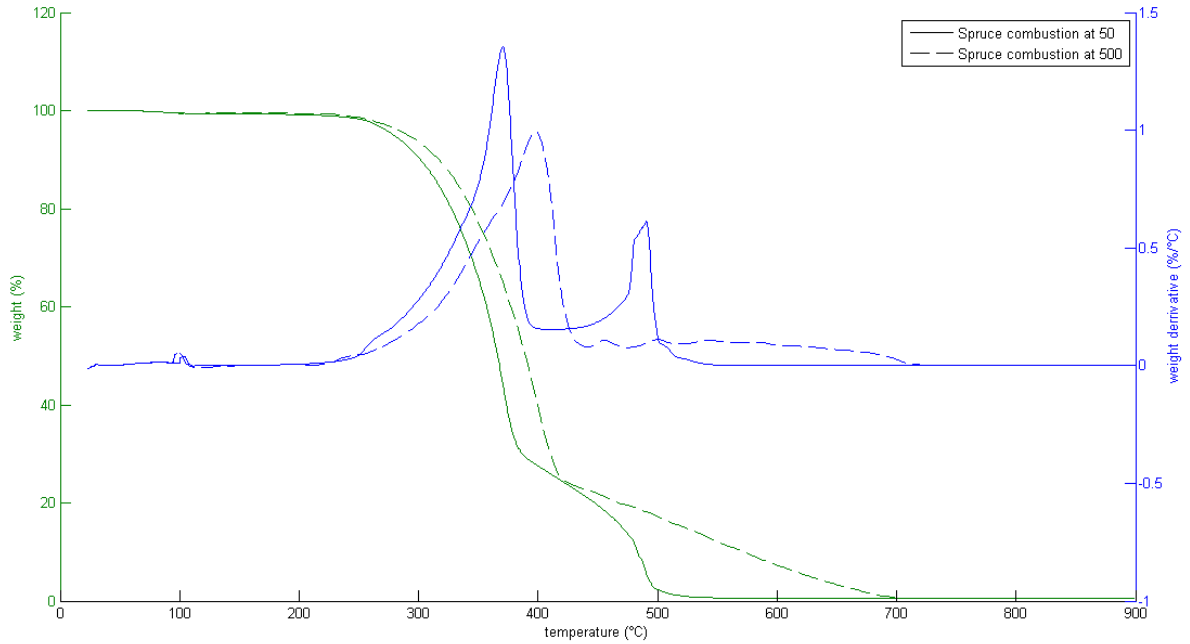

FIGURE 5.1 TGA DATA SPRUCE COMBUSTION AT 50 AND 500 °C/MIN

Around 100 °C, first a small peak corresponding to the drying of the sample occurs in both experiments, Figure 5.1. Furthermore, two stages in the combustion process are recognized. The first stage of combustion has a peak in the DTG graph at 370-400 °C, depending on the heating rate. The

second stage of combustion creates a peak around 490°C for the low heating rate and a broader region between 450-700 °C for a heating rate of 500 °C/min.

For the slow heating rate (50 °C/min) during the first stage of combustion volatiles are removed from the sample and possibly burn; during the second stage of combustion the remaining char oxidizes. [10], [34] For a higher heating rate (500 °C/min) the first stage of combustion is shifted to higher temperatures, which is partly caused by a delay in heat and mass transfer due to the high heating rate used. Even with the relatively small particles used, a temperature gradient is expected to be present inside the particles during heating at these speeds. Furthermore, volatiles released inside the particle will need some time to diffuse outside the particle, which is expected to have an influence at these short heating times. Moreover, the second stage of combustion is spread out over a larger temperature region, which is also expected to be mainly caused by heat and mass transfer limitations at this high heating rate.

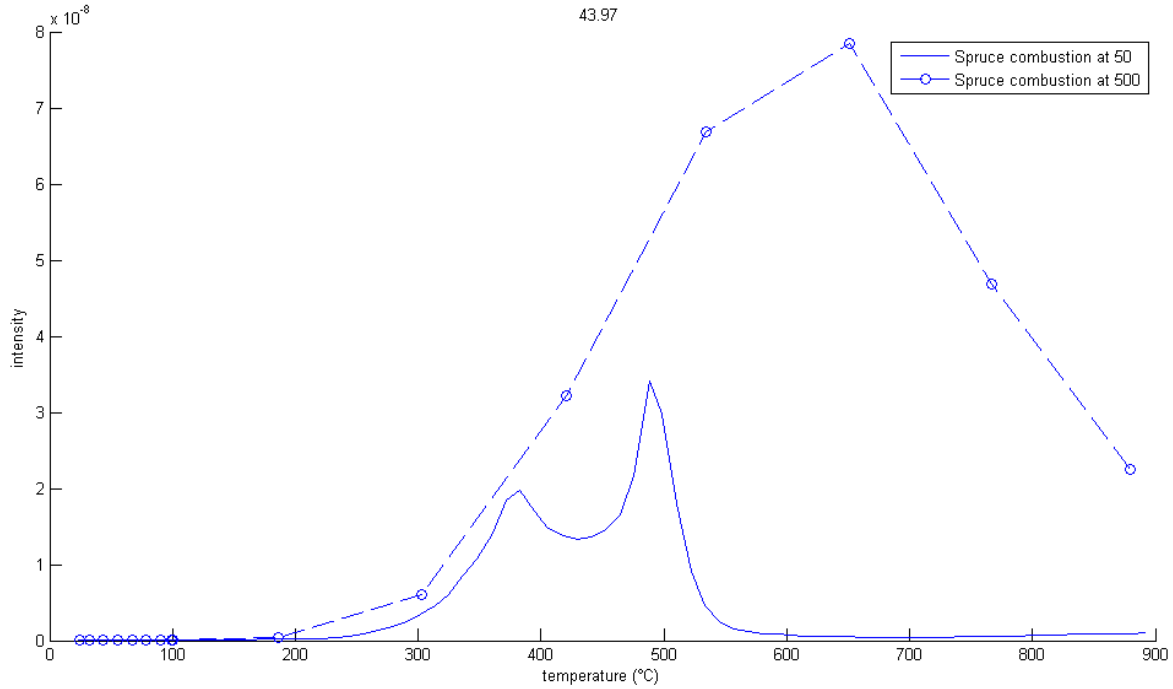

FIGURE 5.2 MS DATA MASS 44 SPRUCE COMBUSTION AT 50 AND 500 °C/MIN

In the MS data (Figure 5.2) for low heating rate (50 °C/min) both the first and second stage of combustion can be recognized in the intensity of m/z ratio 44, which corresponds to the presence of carbon dioxide. The first peak occurs at 380 °C and the second peak at 490 °C. This matches quite well with the first and second stage of combustion in the TGA data (which shows peaks in the DTG graph at 370 and 490 °C). Also in the FTIR data of slow spruce combustion two carbon dioxide peaks in time are recognized.

For higher heating rates the sample time of the MS (approximately 14 seconds), plays a significant role. Therefore, the gas release at high heating rate resulted in just one peak, with few data points and the accuracy of the temperature decreases dramatically. At this high heating rate, gasses are released within a shorter time, resulting in a higher concentration and higher intensity in the MS data. Furthermore, the two experiments in Figure 5.2 do not have the same timeline. Therefore no quantative comparison can be made. When intensity is plotted versus time, it is observed that approximately the same amount of CO_2 is formed.

Gas product during combustion

From the MS data it shows that water (18), aldehydes (30), carbon dioxide (44), organic acids (46), propanal (58) and furan (68) are formed during spruce combustion at both heating rates. At the high heating rate, also m/z ratio 15, corresponding to methane or methyl groups, shows a peak. As mentioned before, concentration of species will be higher when a higher heating rate is applied. From the FTIR data the presence of water and carbon dioxide is clearly visible, furthermore small amounts of hydrocarbons, carbohydrates, acids and phenols are visible.

It can be concluded that no complete combustion of the sample has occurred, because the gasses are purged away to lower temperatures, not allowing complete combustion reaction in this TGA setup. Otherwise the main products would be water and carbon dioxide.

5.3 Influence of heating rate on spruce pyrolysis

In Figure 5.3, TG and DTG data from spruce pyrolysis at 50 and 500 °C/min is plotted.

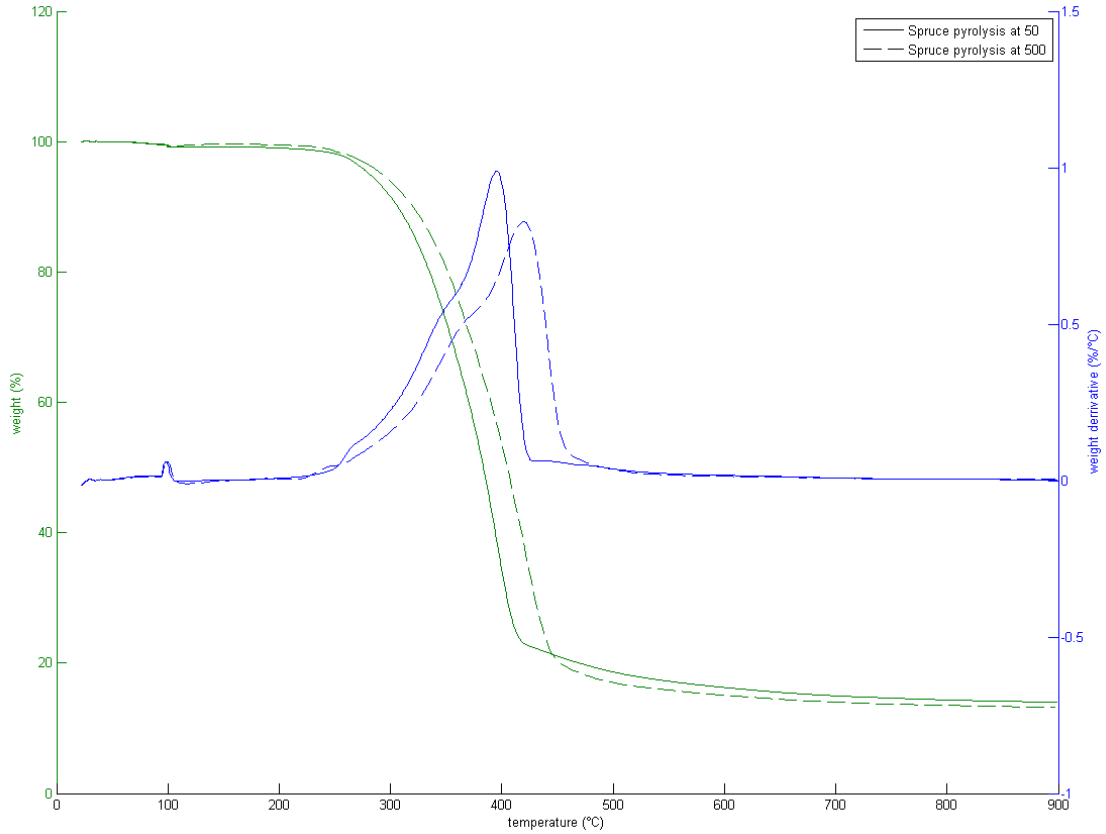

FIGURE 5.3 TGA DATA SPRUCE PYROLYSIS AT LOW AND HIGH HEATING RATE

Once more, a peak corresponding to the drying of the sample is visible around 100 °C for both experiments. After that the main weight loss peak, including a slight hemi-cellulose shoulder, is visible. For the higher heating rate, the main weight loss peak is shifted to a higher temperature (+25 °C) and the peak decreases slightly in height. Due to the expected influence of heat and mass transfer at this high heating rate, no conclusions can be drawn about reactivity for the pyrolysis experiment itself. To investigate the reactivity of the remaining char after pyrolysis, both produced chars have been combusted and gasified using the same method.

A slight but significant difference in final char yield after pyrolysis at the two applied heating rates was present (Figure 5.4). On average 14.1 % char was formed at low heating rate and 13.3 % char at high heating rate (both at a dry weight base).

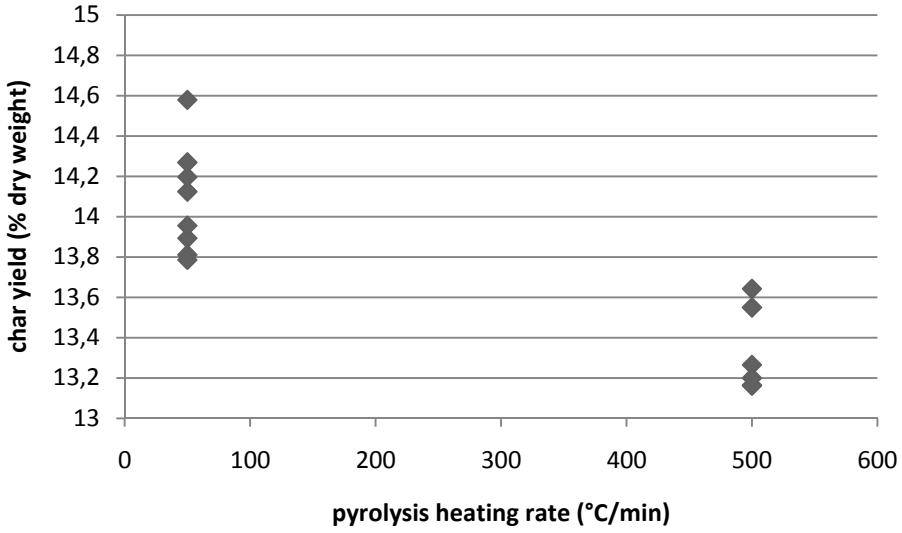

FIGURE 5.4 CHAR YIELD DEPENDING ON HEATING RATE

Gas product during pyrolysis

During pyrolysis the following species were detected by the MS: methane or methyl groups (15), water (18), aldehydes (30), carbon dioxide (44), organic acids (46), propanal (58), hydroxyaldehyde (60) and furan (68). Gas products visible in the FTIR during pyrolysis experiments are water, hydrocarbons, carbon dioxide, carbon monoxide, acids and carbonyl groups and carbohydrates, acids and phenols. Component type of evolved species matches in MS and FTIR data.

As expected, there is a clear product gas difference between combustion and pyrolysis, especially visible in the FTIR data. Carbon monoxide, acids and carbonyl groups are showing during pyrolysis and not during combustion. Furthermore, more hydrocarbons, carbohydrates, acids and phenols are present in the product gas. Concluding, during pyrolysis larger amounts of large molecules have been detected (especially by the FTIR), which have been further oxidized during combustion.

Char production

Various experiments using char as a sample have been performed. These chars have been produced by the pyrolysis process, as described above. The two types of char used will be referred to as char-50 and char-500. Char-50 has been produced by applying pyrolysis to the original spruce sample at a heating rate of 50 °C/min and char-500 with a heating rate of 500 °C/min, the final temperature was similar, 900 °C, during both char productions. And in between char production and the subsequent experiment, the furnace chamber was kept closed to limit external influences. The sample was allowed to cool down in nitrogen atmosphere until the temperature reached below 50 °C. Then the gasses were switched to CO_2 and N_2 (gasification), air (combustion) or the char was preserved for SEM picture (section 5.5.3). The furnace chamber was purged for at least 30 minutes before starting the subsequent experiment.

The reproducibility of the char production was checked and TGA and MS data is considered reproducible for all experiments. In the FTIR the spectra at maximum gas release match quite well, except for the amounts of water and carbon dioxide, which are showing unexplainable behaviour over time due to an error in the FTIR equipment.

5.4 The char gasification process

In Figure 5.5 the gasification of char produced at low heating rate (50 °C/min) is visualised. Curves plotted are weight (%, green), weight derivative (%/min, blue) and temperature (°C, red), all as a function of time (min).

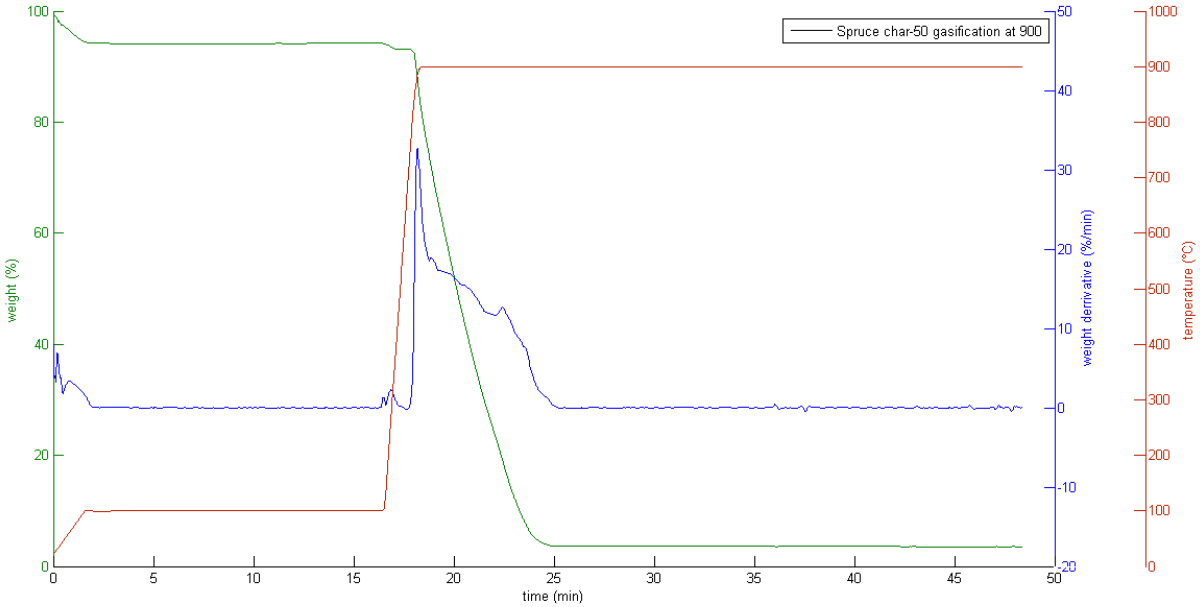

FIGURE 5.5 TGA DATA LOW HEATING RATE CHAR GASIFICATION AT 900 °C

From Figure 5.5 three weight loss regions can be noticed, first between 0 and 2 min, second between 16 and 17.5 min and third between 17.5 and 25 minutes.

Normally, the first weight loss stage at low temperatures can be explained by drying of the sample, but in this case it is highly unlikely that there is still any moisture present in the char sample. Char is a highly reactive substance and easily binds gasses to its surface, for example, ultra clean char surfaces can already adsorb oxygen molecules at room temperatures [26] and also nitrogen adsorption on char surface has been observed. [36] Therefore, it is suggested that this weight loss is caused by desorption of CO_2 or N_2 molecules, that have absorbed on the surface during the purging of the gasses.

The second weight loss phase occurs when the temperature is increased after the drying phase around pyrolysis temperatures. But since the char was prepared with a method reaching 900 °C, it is expected that most volatiles have already been removed from the sample.

DeGroot and Shafizadeh [37], have investigated gasification kinetics of wood char gasification with CO_2. They prepared chars by keeping them 10 min isothermal at 1000 °C and stored them in a storage desiccator under reduced pressure. For the gasification, chars were heated up to 950 °C under nitrogen and when this temperature was reached carbon dioxide was added to the gas stream. At elevated temperatures, before adding the CO_2, some weight loss was observed, which they

explain by a small degree of pyrolytic gasification, due to the gasification of oxidized surface species formed during storage and handling of the char.

Kannan and Richards [38] investigated the influence of the indigenous metal content of biomass chars on the gasification rate during carbon dioxide gasification. They prepared chars at 750 °C with 10 min isothermal stage and stored the chars in desiccators under nitrogen. During the gasification experiments, temperature was raised up to 750 °C and kept at this temperature for 5.5 min before adding CO_2 to the gas stream. They observed a rate of pyrolysis prior to gasification and before adding CO_2 to the gas stream.

Further devolatilization during the current experiments is considered highly unlikely, because the char was prepared immediately before gasification, no storage phase was present and the furnace chamber was kept closed between the preparation and gasification of the char. Although, a specific cause for the pre-gasification weight loss cannot be pointed out, it is sure that this weight loss is not caused by a gasification reaction. Since gasification reactions between carbon dioxide and char have only been reported to occur at higher temperatures [4] and this pre-gasification weight loss ends when the temperature is approximately 650 °C.

It can be concluded that the first two weight loss stages are not a part of the gasification process itself, so during the rest of the discussion of the gasification data, the reader is asked to focus on the main weight loss peak, corresponding to the gasification process.

The main weight loss takes in this experiment approximately 7.5 minutes. The weight loss is faster at the start of the gasification and gets slower when more char has been converted, Figure 5.5. The reaction rate decreases with increasing char conversion, which has been observed for all gasification experiments.

Gas product during char gasification

In the MS data, only mass 60 is showing a peak during char gasification when applying one of the methods, but it lasts only a short time and only shows during one method. Therefore, its behaviour is not considered representative for the gasification process.

Although, the data gained from the FTIR during char gasification experiments was not reproducible (especially at carbon dioxide and water wave numbers), in every char gasification experiment the formation of carbon monoxide was visible.

During the preparation of the char, already the majority of the hydrogen and oxygen present in the feedstock has been removed and resulted in carbon rich char. Not many other species are expected to evolve during char gasification, which is supported by this data.

Finally, it can be concluded from the FTIR data that some carbon monoxide is formed during CO_2 char gasification, but no quantitative conclusions can be drawn.

5.5 Char reactivity

To investigate the influence of applied heating rate during pyrolysis on char reactivity, multiple gasification and combustion experiments with the two char types as sample were performed. Furthermore, scanning electron microscope pictures were taken of char-50 and char-500.

5.5.1 Char gasification reactivity

In Figure 5.6, the gasification at 900 °C of low (char-50) and high (char-500) heating rate char is visualized. It is observed that both chars behave similar until 17.5 minutes (T=700 °C). After that char-500 is losing weight faster (weight derivative is larger) and the gasification finishes 1.5 minutes earlier than the gasification of char-50. Similar behaviour is observed when performing gasification of both chars at 50 °C/min up to 900 °C and 'isothermal' gasification at 800 °C.

Concluding, in all used methods, the high heating rate char is more reactive towards gasification compared to low heating rate char.

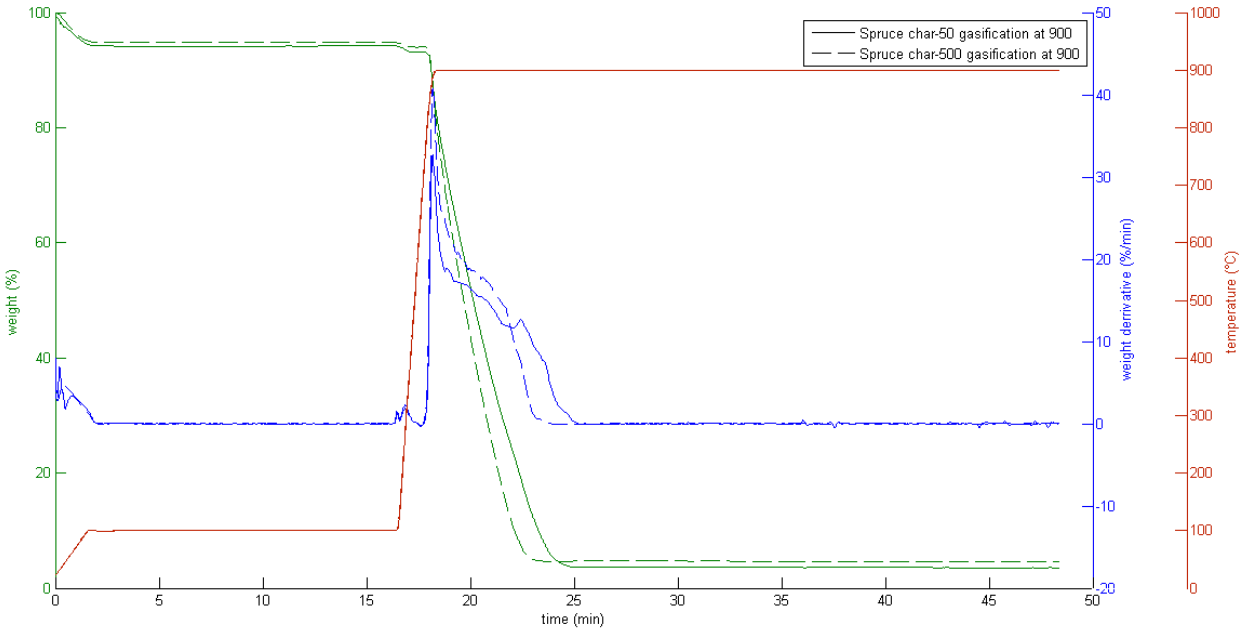

FIGURE 5.6 CHAR GASIFICATION REACTIVITY AT 900 °C

5.5.2 Char combustion reactivity

To investigate the influence of applied heating rate during pyrolysis on char reactivity towards combustion two char combustion experiments were performed and the results compared. It was concluded that low heating rate char was slightly more reactive towards combustion compared to high heating rate char. This result was not in agreement with the char gasification reactivity experiments (previous section), nor in agreement with literature [33] [34] [39]. Therefore, both char combustion experiments were reproduced. The combustion of high heating rate char was reproducible (a difference in starting temperature of the weight loss of maximum 5 °C), but, the combustion of low heating rate char was not reproducible (a difference in starting temperature of the weight loss of approximately 30 °C). To ensure which one of the low heating rate char combustion experiments was right and which one was wrong, this experiment was reproduced one more time. This led to the conclusion that the results from the first performed char-50 combustion were not in agreement with the expected behaviour.

Finally, the trustable data of low and high heating rate char combustion is plotted in Figure 5.7, in which combustion of both char was performed using the same method at a heating rate of 50 °C/min.

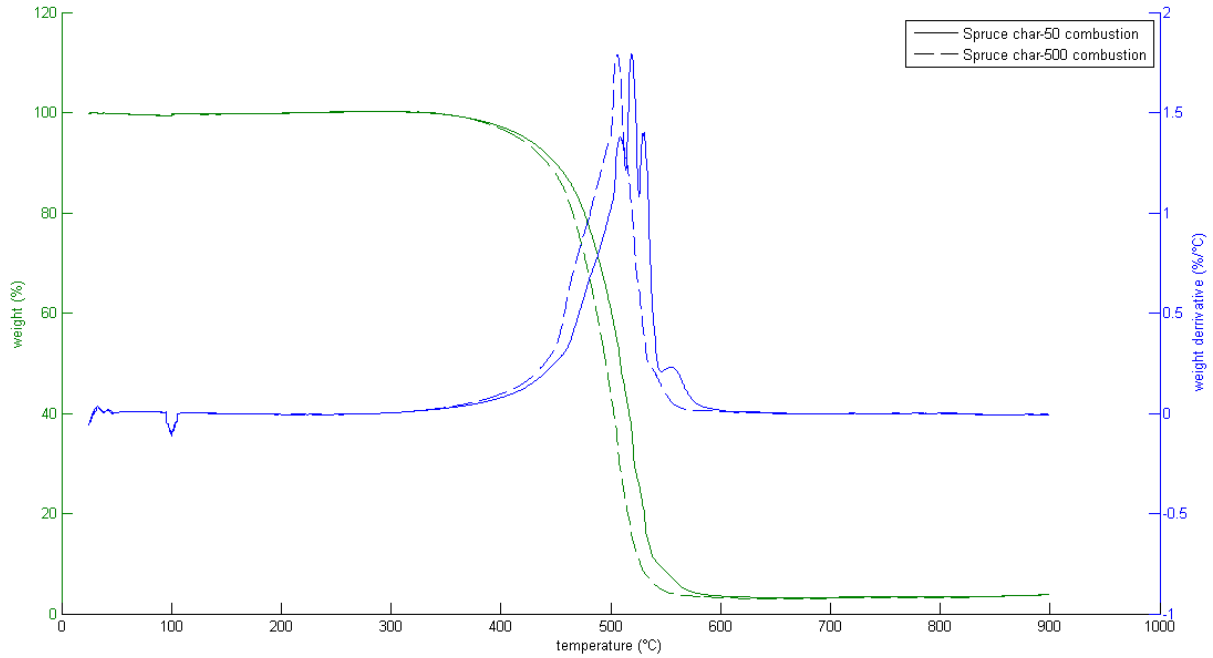

FIGURE 5.7 CHAR COMBUSTION REACTIVITY

During the drying stage, 15 min at 100 °C, the weight of the char increased slightly for all char combustion experiments. This weight increase is caused by oxygen adsorption on the char surface. Ultraclean carbon surfaces are known to adsorb oxygen already at room temperatures. [26]

The combustion process of both chars starts around the same temperature, ~350 °C, but char-500 loses weight faster and its combustion is finished 17.5 °C earlier compared to the combustion of char-50. Therefore the reactivity towards combustion of char produced at a high heating rate is higher than char produced at a low heating rate.

5.5.3 SEM pictures

Scanning electron microscope (SEM) pictures were taken from low heating rate char (char-50), high heating rate char (char-500) and the original spruce sample (no heat treatment). A spura 55VP Scanning Electron Microscope produced by Zeiss (Figure 5.8) was operated by Liang Wang, employee at SINTEF Energi AS, to produces pictures with the secondary electron detector. The samples were mounded on the holder with double sided carbon tape (Figure 5.9). The char samples (char-50 and char-500) did not receive any pre-treatment. Without a pre-treatment, the original spruce sample showed too much accumulation of electrons on the surface, resulting in an 'overexposed' picture. Therefore, the surface of the original spruce sample was coated with carbon.

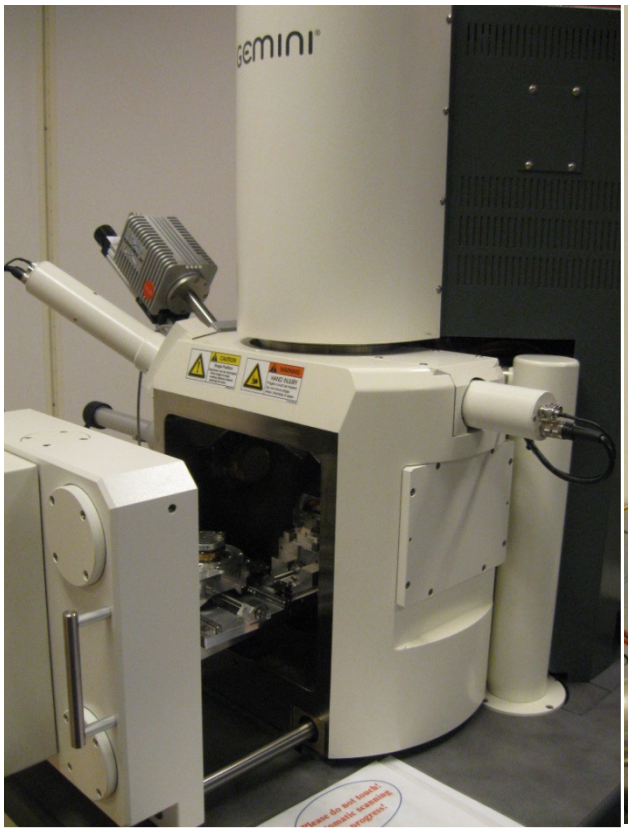

FIGURE 5.8 SCANNING ELECTRON MICROSCOPE

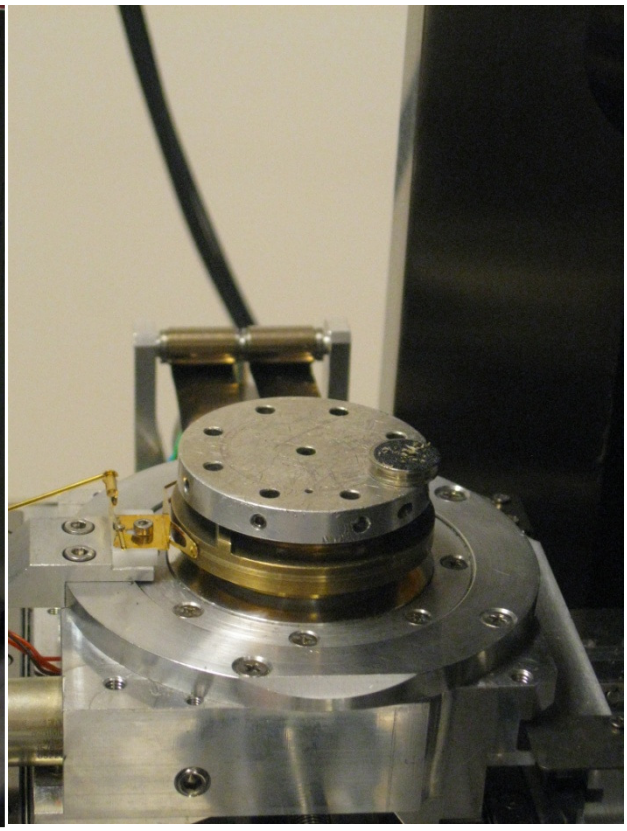

FIGURE 5.9 SAMPLE ON SAMPLE HOLDER FOR SEM

The longitudinal tube structure of wood, as discussed in section 1.1, is clearly recognized in the original spruce sample, Figure 5.10. Also the pits, used to transport water between tracheids, have been observed, inset Figure 5.10. Furthermore, the horizontal orientated cells (perpendicular rays) are not observed on the surface of this particular spruce particle, but have been observed repeatedly on other spruce particles.

The circles in the background of the picture are part of the carbon tape, used to stick the sample onto the holder.

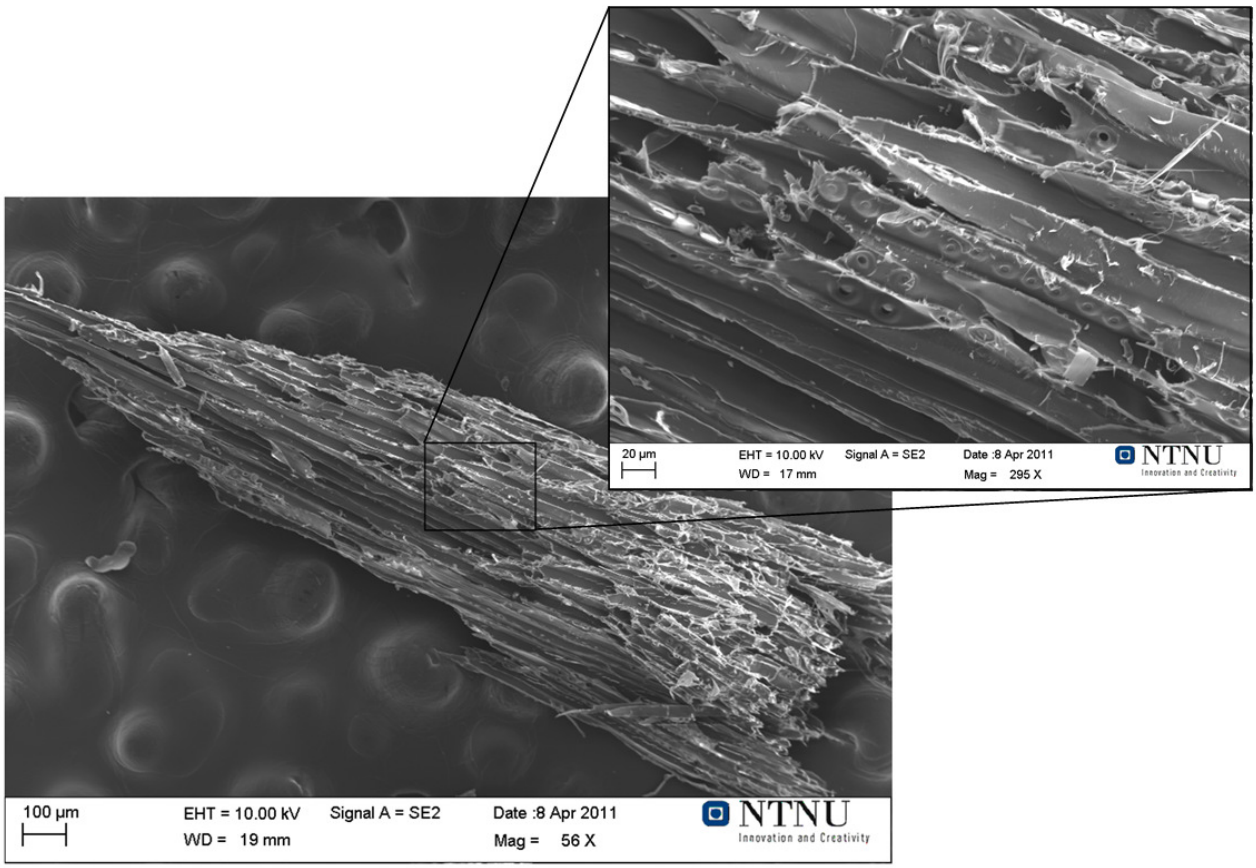

FIGURE 5.10 SEM, ORIGINAL SPRUCE SAMPLE

For both chars (char-50 and char-500) two pictures at two magnifications are shown in Figure 5.11 - Figure 5.14. For both chars, the original structure of the wood is clearly visible and the three structural components observed in the original spruce (longitudinal tracheids, perpendicular rays and pits) are observed.

A comparison between the chars prepared at different heating rates at (approximately) the same magnification is made, it is suggested that char-50 has a more compact structure compared to char-500, because space between longitudinal tracheids seems smaller, the surface of char-50 is flatter and less coarse and char-500 has a more open structure.

A more open structure corresponds to a higher surface area of the char, which is correlated to a higher concentration of carbon active sites. [35] Biomass char combustion and gasification are solid-gas reactions and hence a surface-initiated processes. Therefore, the active site concentration is directly related to the reactivity. [38] This suggests a higher reactivity of high heating rate char compared to low heating rate char.

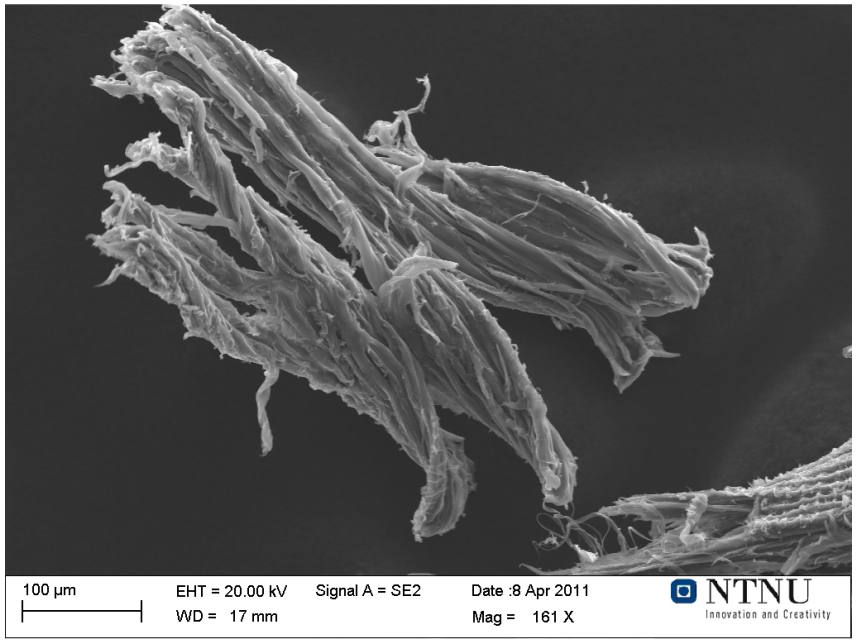

FIGURE 5.11 CHAR PRODUCED AT LOW HEATING RATE (1), WD=17 MM, MAG=161X

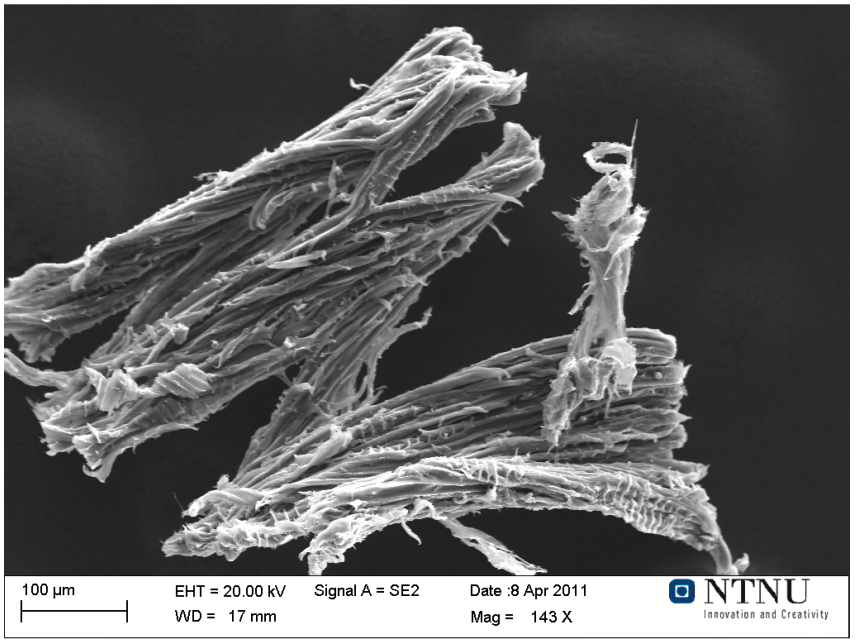

FIGURE 5.12 CHAR PRODUCED AT HIGH HEATING RATE (1), WD=17 MM, MAG=143X

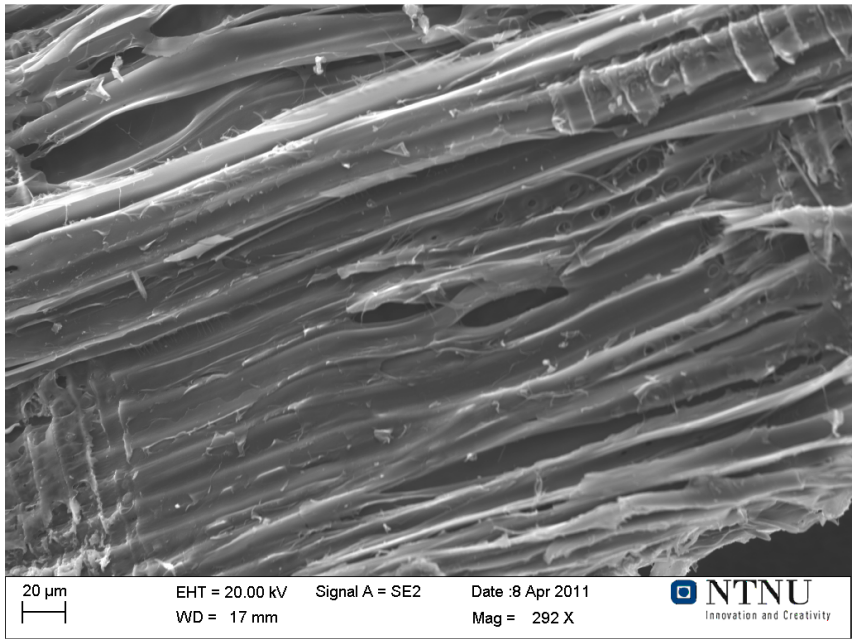

FIGURE 5.13 CHAR PRODUCED AT LOW HEATING RATE (2), WD=17MM, MAG=292X

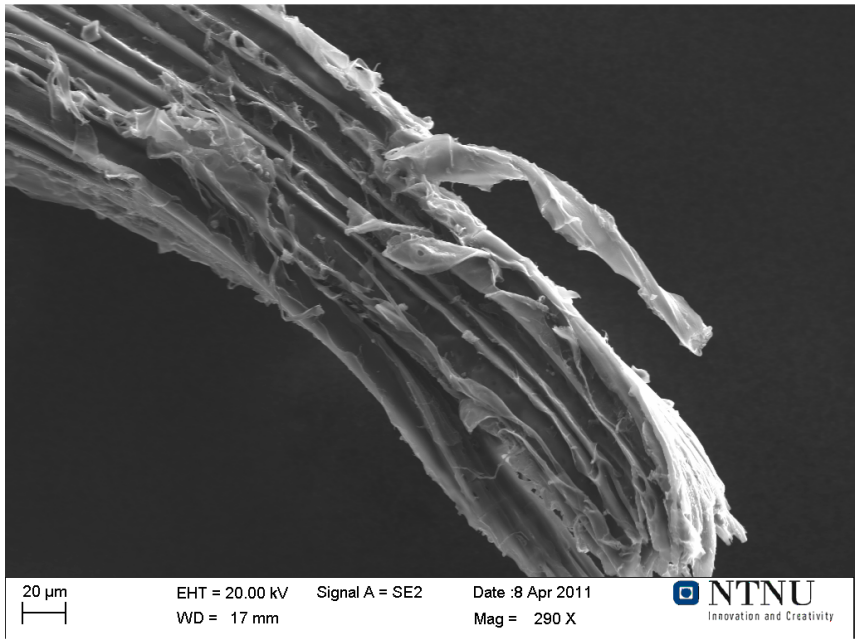

FIGURE 5.14 CHAR PRODUCED AT HIGH HEATING RATE (2), WD=17 MM, MAG=290X

5.6 Influence of gasification temperature

To examine the influence of gasification temperature char-50, char-500 and spruce have been gasified at two different temperatures, 800 and 900 °C. The gasification of char-50 at both temperatures is plotted in Figure 5.15.

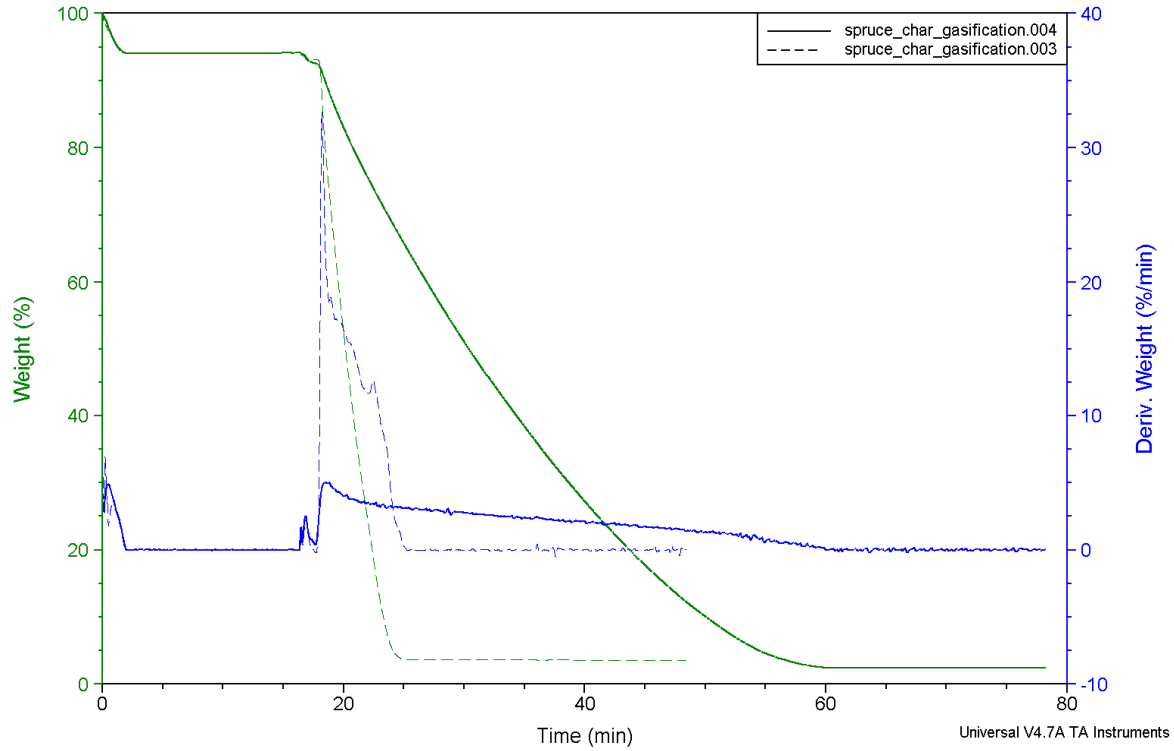

FIGURE 5.15 CHAR-50 GASIFICATION AT 800 °C AND 900 °C

The profile of the main weight loss is similar, both show reduced reaction rate with increased char conversion. As expected, the gasification process at 800 °C takes much longer compared to gasification at 900 °C (~43 and ~7 min, respectively), since gasification reactions happen much slower at lower temperatures.

5.7 Influence of gasification in one or two steps

Direct gasification, without first producing char, was applied to the spruce sample with three different methods, (section 4). For all methods, the process is divided in three stages: drying stage, pyrolysis stage and gasification stage. The results of spruce gasification at 50 °C/min up to 900 °C are shown in Figure 5.16. During the drying stage moisture is removed from the sample. During the pyrolysis stage volatiles are removed from the sample and during the gasification stage the remaining material is reacting with carbon dioxide. For all applied methods, the weight loss during the pyrolysis stage matches very well with the weight loss curves obtained during pyrolysis experiments.

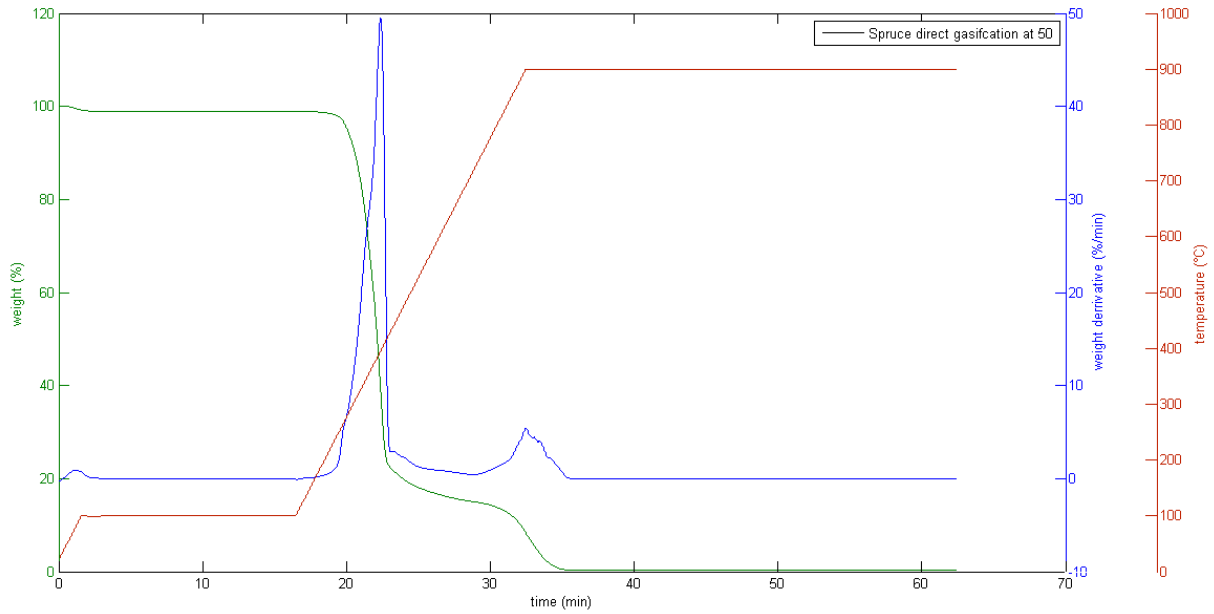

FIGURE 5.16 DIRECT SPRUCE GASIFICATION AT 50°C/MIN

The third stage, gasification, during direct gasification at 50 °C/min has been compared to char-50 gasification at 50 °C/min, Figure 5.17. (The mass of the char has been normalized to the mass of the original spruce sample to make a fair comparison possible.)

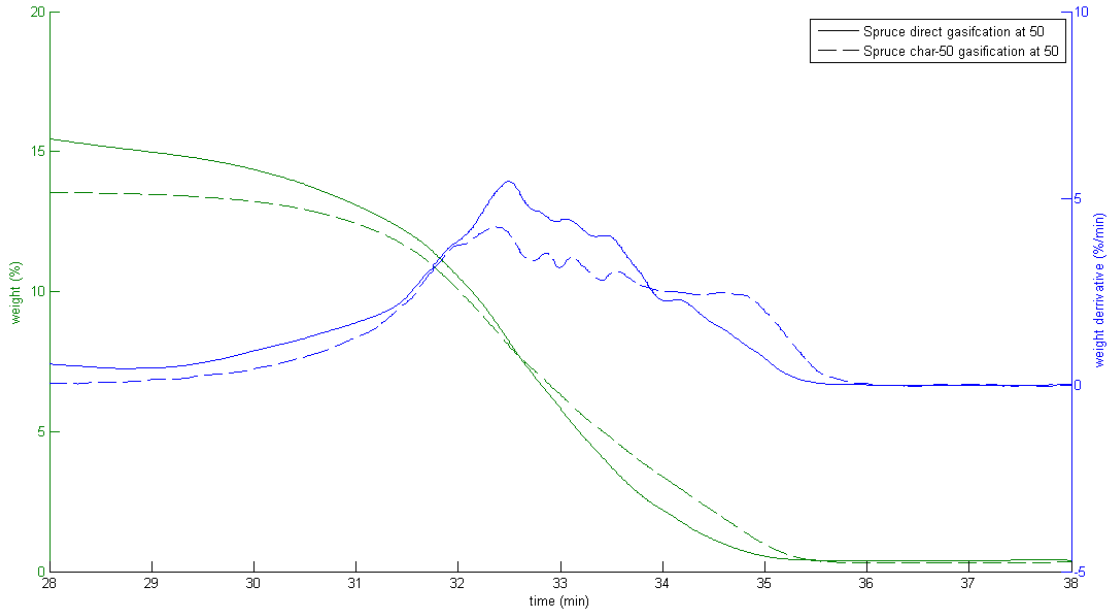

FIGURE 5.17 DIRECT SPRUCE GASIFICATION AND CHAR GASIFICATION AT 50°C/MIN

During direct gasification, the sample is losing weight faster compared to the char and the gasification process is finished earlier (~0.5 min).

When comparing the gasification stage of direct gasification 'isothermally' at 900 °C and char-500 gasification 'isothermally' at 900 °C (Figure 5.18), it also shows that the direct gasification is losing weight faster and is finished earlier than the char(-500) gasification (~ 1 min).

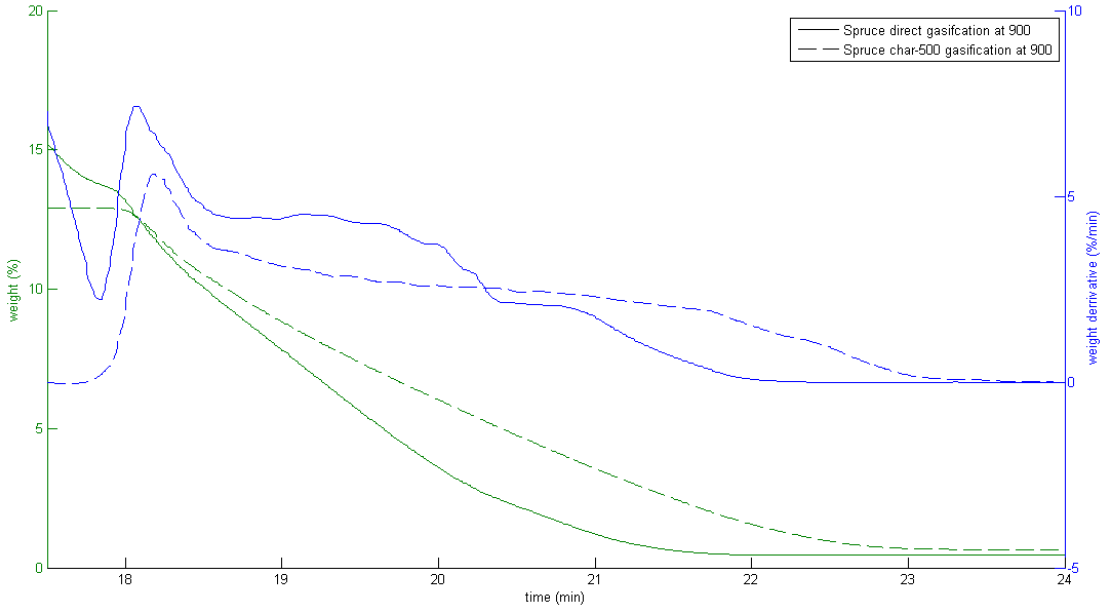

FIGURE 5.18 DIRECT SPRUCE GASIFICATION AND CHAR GASIFICATION 'ISOTHERMALLY' AT 900°C

Concluding, direct spruce gasification is a multi stage process when the methods used in this study are applied. The pyrolysis stage of direct gasification matches to single pyrolysis experiments. But a considerable difference is present between the gasification stage in direct gasification and gasification of char. During the production of the char, after the temperature reached 900 °C the char cools down inside the furnace and is still exposed to relatively high temperatures for some time. Liu *et al.* [40], investigated influence of pyrolysis time on coal char reactivity and concluded that a longer pyrolysis time led to lower reactivity of a char probably due to a structural changes of the char during pyrolysis. It is suggested that during these experiments the char slightly developed further during cooling down, which resulted in a more stable and less reactive structure of the char.

Gas product during direct gasification

In the MS data the origination of methane or methyl groups (15), water (18), aldehydes (30), propanal (58), hydroxyaldehyde (60) and furan (68) is visible during direct gasification. Furthermore, m/z ratio 15 and 60 showed only when a high heating rate was applied and m/z 46 only shows an indication that something is happening, not a clear peak. The FTIR shows evolution of water, hydrocarbons, carbon dioxide, carbon monoxide, acids and carbonyl groups and carbohydrates, acids and phenols and finally carbon monoxide (a bit later than the rest).

Compared to pyrolysis, the origination of carbon dioxide is not showing, since gasification with carbon dioxide is performed. The other species are consistent with first a pyrolysis stage and then a gasification stage.

Concluding, generally species evolved during pyrolysis also show during direct gasification of the spruce sample, confirming the statement that the second stage in direct gasification is similar to pyrolysis. After this stage carbon monoxide, corresponding to the gasification process is formed.

6 Conclusions and recommendations

Influence of heating rate on the gasification process and char reactivity has been investigated by performing multiple gasification, pyrolysis and combustion experiments, using a thermogravimetric analyzer, Fourier transform infrared radiation analyzer and a mass spectrometer.

Problems and set-up evaluation

All used apparatus contributed, to more or less extent, to the gaining of insight of the gasification process. Due to unsolved and unexplained noise problems in the FTIR, its added value to the current study is small, but it has a large potential.

The results gained from the MS were limited, partly due to change in amplification factor, partly because it was not calibrated and partly because the transfer line between FTIR and MS was not insulated. The change in amplification factor of the detector and the fact that the MS was not calibrated, resulted in the fact that nothing could be said about amounts of species evolved, when comparing two experiments. The MS was very useful in proving the incorrectness of the FTIR results by eliminating influence of external events. The MS was capable to show for example clear peaks of carbon dioxide during experiments, were the FTIR was showing increase, decrease or noise of absorbance at carbon dioxide wave numbers. The non heated transfer line probably allowed components in the product gas to condense inside the line, making them undetectable in the MS.

The TGA (when it was fixed and no noise was present in the data anymore) was very useful to observe different stages of weight loss within an experiment and compare reactivities between experiments.

Results

When applying a higher heating rate, delays in weight loss were noted both in combustion, pyrolysis and gasification. Cause of this delay is expected to be heat and mass transfer limitations, but other causes cannot be eliminated.

The char gasification process contained two weight loss stages not belonging to the gasification process. The first is expected to be caused by influence of desorption phenomena, for the second stage no convincing explanation was found, but it is sure this stage is not a part of the gasification reactions. The main gasification stage, both in char and direct gasification, was characterized by a weight loss that got smaller when there was less weight left (reduced reaction speed with increasing conversion). When lowering the gasification temperature, the gasification reaction decreased much in speed. By comparing gasification in one or two steps, it showed that the gasification stage in the two steps process took a little longer, indicating further structural development of the char during cooling down after char production.

Char reactivity has been examined by scanning electron microscope (SEM) pictures, char combustion experiments and gasification experiments. Char gasification clearly showed higher heating rate char to be more reactive. After some irreproducible experiments, also char combustion resulted in the same conclusion. From the SEM pictures it was suggested that the high heating rate char was likely to be more reactive. It can be concluded that in all examined situations char produced at a higher heating rate is more reactive than lower heating rate char.

Recommendations

To gain more information about the composition of the product gas, it is recommended to use another inert gas to purge then nitrogen, for example argon (40 amu) or helium (4 amu). This would result in the capability to observe carbon monoxide in the MS.

The non heated transfer line between the FTIR and the MS probably allowed components in the product gas to condense inside the line. Therefore, when experiments will be continued including the MS, it is recommended to insulate the transfer line between the FTIR and the MS.

Heat and mass transfer effects are expected to be causing delays in weight loss when increasing the heating rate. Since heat and mass transfer effects are directly related to particle size, it is recommended to reproduce similar experiments with significantly smaller particles. It is expected that in these future experiments, delays will be smaller, thus confirming the influence of heat and mass transfer. It is expected that heat and mass transfer influence cannot be totally eliminated by reducing the particle size, because of the very high heating rate applied (500 °C/min).

During direct spruce gasification at high heating rate (500 °C/min), the processed of pyrolysis and gasification were still separated. It can be interesting to try a direct gasification experiment with a ballistic heating rate. Then the TGA can heat up to the desired temperature at >2000 °C/min, which might result in combining the pyrolysis and gasification stage and make the experiment more similar to situations in a real gasifier.

7 Bibliography

1 Grønli MG. A theoretical and experimental study of the thermal degradation of biomass. Doctoral Thesis. Trondheim: The Norwegian University of Science and Technology; 1996. NTNU 1996:115.

2 Bastiaans dR, Oijen dJ, Prins dM. Energy from biomass. Enschede: University of Twente; 2005. 4S610.

3 Kögel-Knabner I. The macromolecular organic composition of plant and microbial residues as inputs to soil organic matter. Soil Biology & Biochemistry. 2002;34:139-162.

4 Matas Güell B. Design of efficient catalysts for steam reforming op pyrolysis oil to hydrogen. Enschede: Gildeprint; 2009.

5 Zhang L, Xu C, Champagne P. Overview of recent advances in thermo-chemical conversion of biomass. Energy conversion and management. 2010;51:969-982.

6 Müller-Hagedorn M, Bockhorn H, Krebs L, Müller U. A comparative kinetic study on the pyrolysis of three different wood species. Journal of analytical and applied pyrolysis. 2003 231-249.

7 Faix O, Meier D, Fortmann I. Thermal degradation products of wood, A collection of electron-impact (EI) mass spectra of monomeric lignin derived products. Holz als Roh- und Werkstoff. 1990;48:351-354.

8 Wikipedia. [Internet]. [cited 2011 February 25]. Available from: http://en.wikipedia.org/.

9 IEA (EA. Biomass combustion and co-firing: An overview. IEA, (International Energy Agency); 2002.

10 Fang M, Shen D, Li Y, Luo Z, Cen K. Kinet study on pyrolysis and combustion of wood under different oxygen concentrations by using TG-FTIR analysis. Journal of analytical and applied pyrolysis. 2006;77:22-27.

11 Kirkubakaran V, Sivaramakrishnan V, Nalini R, Sekar T, Premalatha M, Subramanian P. A review on gasification of biomass. Renewable and sustainable energy reviews. 2009;13:179-186.

12 Gasifier camp stove. [Internet]. 2010 [cited 2011 February 11]. Available from: http://www.gasifiercampstove.com.

13 Laan Gvd. [Internet]. 1999 [cited 2011 January 31]. Available from: http://dissertations.ub.rug.nl/FILES/faculties/science/1999/g.p.van.der.laan/c1.pdf.

14 Matas Güell B, Sandquist J. Biomass gasification technologies [Internet]. 2011 February.

15 Lucas C, Szewczyk D, Blasiak W, Mochida S. High-temperature air and steam gasification of densified biofuels. Biomass and Bioenergy. 2004;27:563-575.

16 Hernández JJ, Aranda-Almansa G, Bula A. Gasification of biomass wastes in an entrained flow gasifier: Effect of the particle size and residence time.. Fuel Processing Technology. 2010;91:681-692.

17 Umeki K, Yamamoto K, Namioka T, Yoshikawa K. High temperature steam-only gasification of woody biomass. Applied Energy. 2010;87:791-798.

18 Gil J, Corella J, Aznar MP, Caballero MA. Biomass gasification in atmospheric and bubbling fluidized bed: Effect of the type of gasifying agent on the product distribution. Biomass and bioenergy. 1999;17:389-403.

19 Instruments T. TA Instruments: Q5000IR. [Internet]. 2008 [cited 2011 February 4]. Available from: http://www.tainstruments.com/product.aspx?id=82&n=1&siteid=11.

20 Wang L. Method for determination of devolatilization and char reactivity of biomass and waste. Technical report. SINTEF Energi AS; 2010.

21 Cagnon B, Py X, Guillot A, Stoeckli F, Chambat G. Contribution of hemicellulose, cellulose and lignin to the mass and the porous properties of chars and steam activated carbons from various lignocellulosic precursors. Bioresource technology. 2009;100:292-298.

22 Sun L, Chen JY, Negulescu II, Moore MA, Collier BJ. Kinetics modeling of dynamic pyrolysis of bagasse fibers. Bioresource technology. 2011;102:1951-1985.

23 scientific T. Nicolet iS10 FT-IR spectrometer. [Internet]. 2007,2008 [cited 2011 February 11]. Available from: http://www.thermoscientific.com/wps/portal/ts/products/detail?navigationId=L10978&categoryId=82243&productId=11961709.

24 Scientific"". Omnic 8.1.11. ToolBook II [Internet].

25 vacuum P. Mass spectrometer. 2005.

26 Bradbury A, Shafizadeh F. Role of oxygen chemisorption in low-temperature ignition of cellulose. Combustion and flame. 1980;37:85-89.

27 Bassilakis R, Carangelo R, Wójtowicz M. TG-FTIR analysis of biomass pyorlysis. Fuel. 2001;80:1765-1786.

28 Court RW, Sephton MA. Quantitative flash pyrolysis Fourier transform infrared spectroscopy of organic materials. Analytica Chimica Acta. 2009;639:62-66.

29 Thipkhunthod P, Meeyoo V, Rangsunvigit P, Rirksomboon T. Describing sewage sludge pyrolysis kinetics by a combination of biomass factions decomposition. Journal of Analytical and Applied Pyrolysis. 2007;79:78-85.

30 Wang D, Xiao R, Zhang H, He G. Comparison of catalytic pyrolysis of biomass wiith MCM-41 and Cao catalysts by using TGA-FTIR analysis. Journal of Analytical and Applied Pyrolysis. 2010;89:171-177.

31 Thermo Scientific. OMNIC User's Guide, version 8.0. Thermo Fischer Scientific Inc., Madison WI 53711; 2008. 269-032217, Rev A.

32 Di Blasi C. Combustion and gasification rates of lignocellulosic chars. Progress in Energy and COmbustion Science. 2009;35:121-140.

33 Cetin E, Moghtaderi B, Gupta R, Wall T. Influence of pyrolysis conditions on the structure and gasification reactivity of biomass chars. Fuel. 2004;83:2139-2150.

34 Yurdakul S, Atimtay AT. Investigation of combustion kinetics of treated and untreated waste wood samples with thermogravimetric analysis. Fuel processing technology. 2009;90:939-046.

35 Vanvuka D, Karouki E, Sfakiotakis S. Gasification of waste biomass chars by carbon dioxide via thermogravimetry. Part I: effect of mineral matter. Fuel. 2011;90:1120-1127.

36 Hshieh F, Richards G. Factors influencing chemisorption and ignition of wood chars. Combustion and flame. 1989;76:37-47.

37 DeGroot WF, Shafizadeh F. Kinetics of gasification of Douglas Fir and Cottonwood chars by carbon dioxide. Fuel. 1984;63:210-216.

38 Kannan M, Richards G. Gasification of biomass chars in carbon dioxide: dependence of gasification rate on the indigenous metal content. Fuel. 1990;69:747-753.

39 Kumar M, Gupta RC. Influence of carbonization conditions on the gasification of acacia and eucalyptus wood chars by carbon dioxide. Fuel. 1994;73:1922-1924.

40 Liu H, Keneko M, Luo C, Kato S, Kojima T. Effect of pyrolysis time on the gasification reactivity of char with CO2 at elevated temperatures. Fuel. 2004;83:1055-1061.